矿物岩石地球化学通报
Bulletin of Mineralogy, Petrology and Geochemistry
Vol.45 No.2, Mar., 2026

全球不同产出类型铬铁矿的特征及成因讨论

谢慧丹[1],桂维彬[1],龚小晗[2],何亮[3,4],邱添[1],徐向珍[1],杨经绥[1,5],熊发挥[1]*

1. 深地探测与矿产勘查全国重点实验室,中国地质科学院 地质研究所 地幔研究中心,北京 100037; 2. 中国地质大学(北京),北京 100083; 3. 成都理工大学 地球与行星科学学院,成都 610059; 4. 西藏自治区地质矿产勘查开发局第六地质大队,拉萨 851400; 5. 南京大学 地球科学与工程学院,南京 210023

摘　要: 铬铁矿是我国稀缺的战略性矿产资源之一,长期依赖进口,其成因机制与地幔演化和构造体制转换密切相关。本文以全球范围内层状、豆荚状、阿拉斯加型和绿岩带型四类主要铬铁矿床为研究对象,系统对比其矿体产状、矿物组合及岩石学、矿物学和地球化学特征,并综合前人数据探讨其成矿机制与构造背景。研究表明,不同类型铬铁矿在成矿环境、岩浆演化过程及物质来源上存在显著差异,其形成受地幔温度、岩石圈结构、构造体制转换以及俯冲流体和氧化还原条件的共同控制,且铬铁矿成矿具有明显的时空分段性,与全球尺度地幔演化和构造格局演变密切相关,这为理解铬元素的深部循环及全球成矿规律提供了重要依据。

关　键　词: 铬铁矿;不同类型;矿物特征;地球演化史

中图分类号: P618.31;P618.33　**文章编号:** 1007-2802(2026)02-0400-27　**doi:** 10.3724/j.issn.1007-2802.20260004

Characteristics and genetic models of major chromitite deposit types worldwide

XIE Hui-dan[1], GUI Wei-bin[1], GONG Xiao-han[2], HE Liang[3,4], QIU Tian[1], XU Xiang-zhen[1], YANG Jing-sui[1,5], XIONG Fa-hui[1]*

1. *State Key Laboratory of Deep Earth and Mineral Exploration, Center of Advanced Research on Mantle, Institute of Geology, Chinese Academy of Geological Sciences, Beijing* 100037*, China;*
2. *China University of Geosciences (Beijing), Beijing* 100083*, China;*
3. *College of Earth and Planetary Sciences, Chengdu University of Technology, Chengdu* 610059*, China;*
4. *The Sixth Geological Brigade, Tibet Bureau of Geology and Mineral Resources, Lhasa* 851400*, China;*
5. *School of Earth Sciences and Engineering, Nanjing University, Nanjing* 210023*, China*

Abstract: Chromitite is one of China's scarce strategic mineral resources and has long been supplied largely through import from abroad. Its genesis is closely linked to the evolution of the mantle and transformation of tectonic setting. In this study, by taking four major types of chromitite deposits including the layered, podiform, Alaskan-type, and greenstone belt–hosted ones in the world as research objects, we have systematically compared their orebody geometries, mineral assemblages, and petrological, mineralogical, and geochemical characteristics, and further discussed their genetic mechanisms and tectonic settings based on the comprehensive analysis of previously published data of those deposits. The research results reveal that there are pronounced differences among various types of chromitite deposits in terms of metallogenic environments, magmatic evolution process, and provenance of ore-forming materials. The formation of these deposits is jointly controlled by the mantle thermal state, lithospheric structure,

收稿编号:2025-0293,2025-12-08 收到,2026-01-03 改回

基金项目:国家重点研发计划项目(2023YFF0804401);国家自然科学基金项目(U2344202,42172069,U2544206,42272048);新一轮找矿突破战略行动科技支撑项目(ZKKJ202418);西藏自治区科技计划项目(XZ202401YD0006-5);中国地质调查局地质调查项目(DD20250102601,DD20242124,DD20221630,DD20240075)

第一作者简介:谢慧丹(2002—),女,硕士研究生,研究方向:矿物学、岩石学、矿床学. email:erer021106@163.com

*通信作者简介:熊发挥(1985—),男,博士,研究员,研究方向:蛇绿岩、铬铁矿和地幔矿物学. email:xiongfahui@126.com

引用此文:

谢慧丹,桂维彬,龚小晗,何亮,邱添,徐向珍,杨经绥,熊发挥. 2026. 全球不同产出类型铬铁矿的特征及成因讨论. 矿物岩石地球化学通报,45(2):400–426

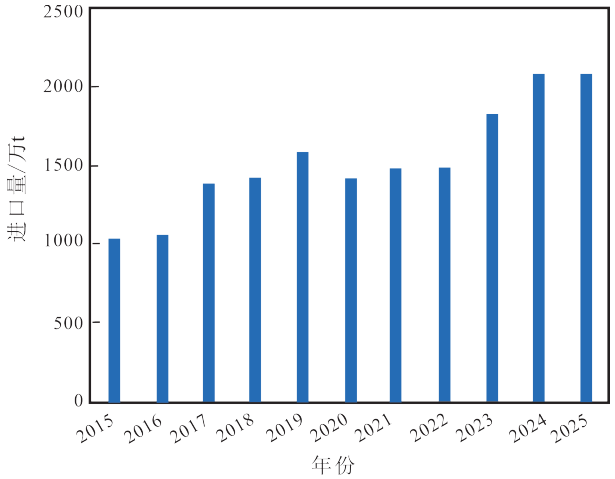
Xie H D,Gui W B,Gong X H,He L,Qiu T,Xu X Z,Yang J S,Xiong F H. 2026. Characteristics and genetic models of major chromitite deposit types worldwide. Bulletin of Mineralogy, Petrology and Geochemistry,45(2):400–426

transformation of tectonic setting, and subduction-related fluids and their redox conditions. In addition, the chromitite mineralization has obvious characteristics of spatiotemporal segmentation and is closely related to the evolution of mantle and tectonic framework at global scale. This research provides important constraints for understanding the cycling of chromium in deep interior of the Earth and the global metallogenic patterns of chromium.

Key words: chromitite; various types; mineral characteristics; evolutionary history of the Earth

0　引言

铬是我国极为关键的战略性矿产资源,因其耐高温、耐磨损、耐腐蚀等特殊属性,广泛应用于建筑业与高端制造业。铬铁矿($FeCr_2O_4$)是自然界中最重要的含铬矿物,也是目前铬可经济利用的唯一来源,但我国铬铁矿资源极度匮乏,长期依赖进口(图1)(张泽南等,2019)。已有研究表明,铬铁矿的形成与地幔的物质组成、深部熔融及岩浆活动密切相关(Thayer,1964;Nicolas,1983;Barnes et al.,2001)。因此,系统研究铬铁矿的成矿机制,不仅是保障关键矿产资源安全的基础,也是揭示地幔演化过程、深部物质循环及岩浆成矿系统耦合关系的重要窗口(杨经绥等,2010,2020)。



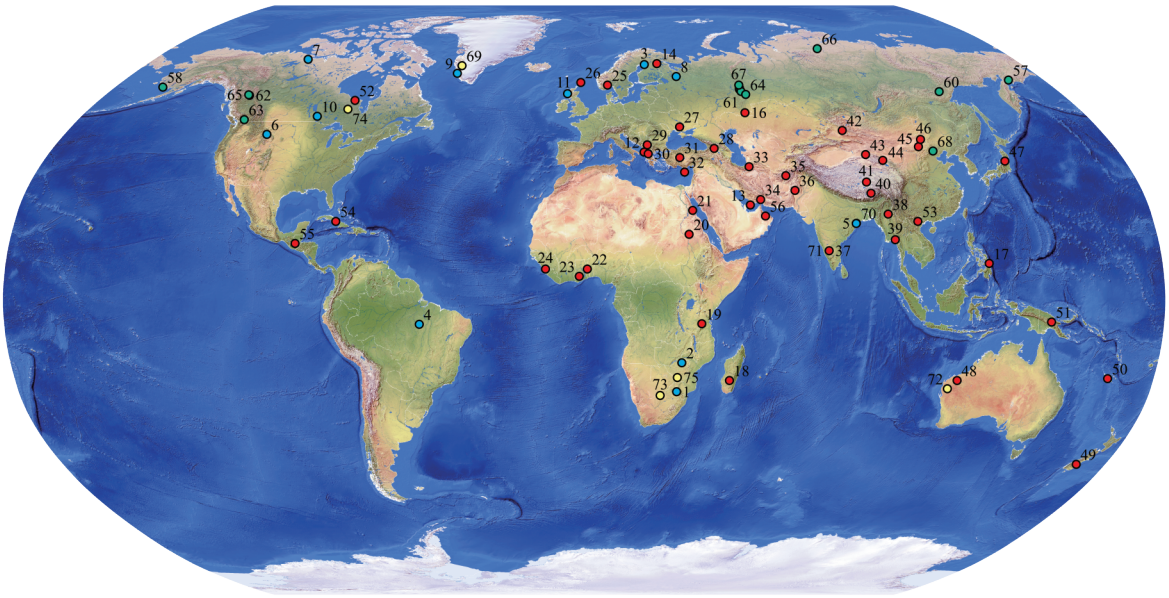
资料来源:中华人民共和国海关总署(2026年统计)

图1　2015—2025年中国铬铁矿进口量

Fig.1　China's imported chromitite volumes from 2015 to 2025

全球铬铁矿床的分布具有显著的空间集聚性,典型表现为在限定区域内形成成矿区(带)(图2),根据其产出的构造背景、含矿岩石组合及矿体形态,主要划分为四大类型(表1):(1)产于稳定克拉通内部或边缘的大型层状镁铁-超镁铁质杂岩体中的层状铬铁矿床(Garuti et al.,2007;Schulte et al.,2012;Marques et al.,2017);(2)产于造山带和岛弧带内蛇绿岩带中的豆荚状铬铁矿床(Mosier et al.,2012;Zhou et al.,2014;Sapanci et al.,2023);(3)产于汇聚板块边缘环带状杂岩体中的阿拉斯加型铬铁矿床(Taylor,1967;Garuti et al.,2003;Zaccarini et al.,2013,2018);(4)产于太古宙克拉通绿岩带内超镁铁质-镁铁质岩体的绿岩带型铬铁矿床(Mondal et al.,2006,2019;Prendergast,2008;Scoates and Jon Scoates,2013)。尽管对铬铁矿的成因已有大量研究,但大数据分析结果显示现有研究多集中于单一类型或局部矿床(Cai et al.,2022),其中层状铬铁矿强调地壳岩浆房内玄武质岩浆的分离结晶、反复补给与晶体堆积过程(Irvine,1975,1977;Spandler et al.,2005;Mondal et al.,2007;Naldrett et al.,2012;Schulte et al.,2012;Latypov et al.,2017);豆荚状铬铁矿突出幔源熔体在上地幔中通道化运移并与寄主橄榄岩之间的反应(Zhou et al.,1994;Arai,1997;Robinson et al.,1997;Zhou et al.,2014;Xiong et al.,2015);阿拉斯加型铬铁矿聚焦于俯冲带上方岛弧-前弧环境中的岩浆过程(Taylor,1967;Himmelberg and Loney,1995;Khedr and Arai,2016;Wang et al.,2023);而绿岩带型铬铁矿则侧重于铬铁矿、岩床状超基性-基性杂岩与高Mg变质火山-沉积建造之间的成因联系(Mondal,2009;Mukherjee et al.,2010,2012;Polat et al.,2010)。这些研究虽然深化了对于单个类型铬铁矿床的认识,但却存在全球铬铁矿成因研究的孤岛化,缺乏一个统一的视角来揭示其成矿物质Cr元素的来源与全球尺度的循环规律,存在的关键科学问题包括:驱动不同类型铬铁矿形成的共同物质基础是什么?铬铁矿的产出是否与地球内部演化过程相关联(Stowe et al.,1994;Coggon et al.,2013)?巨量铬铁矿床的形成,是否预示存在一个更深、更富集的源区(Zirakparvar et al.,2019)?

鉴于此,本文以这四种类型铬铁矿为研究对象,系统梳理其矿体产出特征、矿物组合类型和岩石学、矿物学、地球化学特征及其异同,总结不同类型铬铁矿的成因机制,进而结合全球铬铁矿床成矿年龄与赋存岩体规模数据,分析不同类型铬铁矿的时空分段性及其与壳幔分异、板块构造演化和超级大陆聚散过程的耦合关系,从而约束地幔中铬的富集路径,以期为理解关键铬资源的成矿规律提供科学依据。



● 层状铬铁矿 ● 豆荚状铬铁矿 ● 阿拉斯加型铬铁矿 ● 绿岩带型铬铁矿

1.南非布什维尔德铬铁矿
2.津巴布韦大岩墙铬铁矿
3.芬兰铬铁矿
4.巴西铬铁矿
5.印度奥里萨邦铬铁矿
6.美国斯蒂尔沃特铬铁矿
7.加拿大麝牛铬铁矿
8.俄罗斯布拉科夫斯基铬铁矿
9.格林兰岛菲斯克内塞特铬铁矿
10.加拿大伯德河岩床铬铁矿
11.苏格兰拉姆岛铬铁矿
12.阿尔巴尼亚铬铁矿
13.古勒曼区铬铁矿
14.俄罗斯拉依兹铬铁矿
15.乌拉尔萨拉诺夫铬铁矿
16.乌拉尔肯皮尔赛铬铁矿
17.菲律宾铬铁矿
18.马达加斯加铬铁矿
19.塔桑尼亚铬铁矿
20.苏丹铬铁矿
21.埃及铬铁矿
22.多哥铬铁矿
23.加纳铬铁矿
24.塞拉利昂铬铁矿
25.挪威铬铁矿
26.英国设得兰岛铬铁矿
27.前苏联乌克兰铬铁矿
28.前苏联外高加索铬铁矿
29.南斯拉夫铬铁矿
30.希腊铬铁矿
31.土耳其其它各区铬铁矿
32.塞浦路斯铬铁矿
33.伊朗北部铬铁矿
34.伊朗南部铬铁矿
35.阿富汗铬铁矿
36.巴基斯坦铬铁矿
37.印度迈索尔帮铬铁矿
38.缅甸北部铬铁矿
39.缅甸南部铬铁矿
40.中国西藏罗布莎铬铁矿
41.中国西藏东巧铬铁矿
42.中国新疆萨尔托海铬铁矿
43.中国甘肃肃北铬铁矿
44.中国青海祁连铬铁矿
45.中国内蒙乌盟铬铁矿
46.中国内蒙锡盟铬铁矿
47.日本本州、北海道铬铁矿
48.澳大利亚铬铁矿
49.新西兰铬铁矿
50.新喀里多尼亚铬铁矿
51.新几内亚铬铁矿
52.加拿大铬铁矿
53.越南铬铁矿
54.古巴铬铁矿
55.危地马拉铬铁矿
56.阿曼铬铁矿
57.俄罗斯加尔莫埃南铬铁矿
58.阿拉斯加好新闻铬铁矿
59.乌拉尔卡奇卡纳尔铬铁矿
60.俄罗斯康德尔铬铁矿
61.乌拉尔下塔吉尔铬铁矿
62.加拿大波拉里斯铬铁矿
63.加拿大图拉明铬铁矿
64.乌拉尔乌克图斯铬铁矿
65.芬兰弗雷德铬铁矿
66.俄罗斯古利铬铁矿
67.乌拉尔基特利姆铬铁矿
68.中国高寺台铬铁矿
69.格陵兰岛Ujaragssuit铬铁矿
70.印度苏金达铬铁矿
71.印度阿拉达哈里铬铁矿
72.澳大利亚纽兰兹铬铁矿
73.津巴布韦Railway Block铬铁矿
74.加拿大黑托尔铬铁矿
75.津巴布韦Valley铬铁矿

图2 全球主要铬铁矿矿床分布图(据熊发挥等,2013修编)

Fig.2 The distribution of major chromitite deposits in the world (modified after Xiong F H et al.,2013)

1 全球铬铁矿矿体产出特征

四类铬铁矿床在岩石组合和矿体特征上既存在共性,又存在显著差异(表1,图3)。其中,层状铬铁矿通常与大型层状镁铁-超镁铁质侵入体共生,其岩石组合呈现完整的岩浆分异序列,可划分为下部超基性的纯橄岩序列和上部基性的辉石岩序列,包括纯橄岩、方辉橄榄岩、二辉橄榄岩、辉石岩、橄长岩、苏长岩、辉长苏长岩、斜长岩、斜方辉石岩和辉绿岩(Schulte et al.,2012;Smith and Maier et al.,2021)。岩体中的铬铁矿常呈层状、似层状产于堆晶辉石岩(如Bushveld岩体)或方辉橄榄岩(如Stillwater杂岩体和Great dyke)中,常呈交替互层出现,为典型的火成堆晶层理。单铬铁矿层厚度变化较大,从数厘米到数米不等,侧向延伸可达数十至数百千米(Cawthorn,2005;Schulte et al.,2012)。矿体整体规模大、品位较高,且受后期构造变形影响相对较弱,反映长期、相对稳定的浅部岩浆房环境。

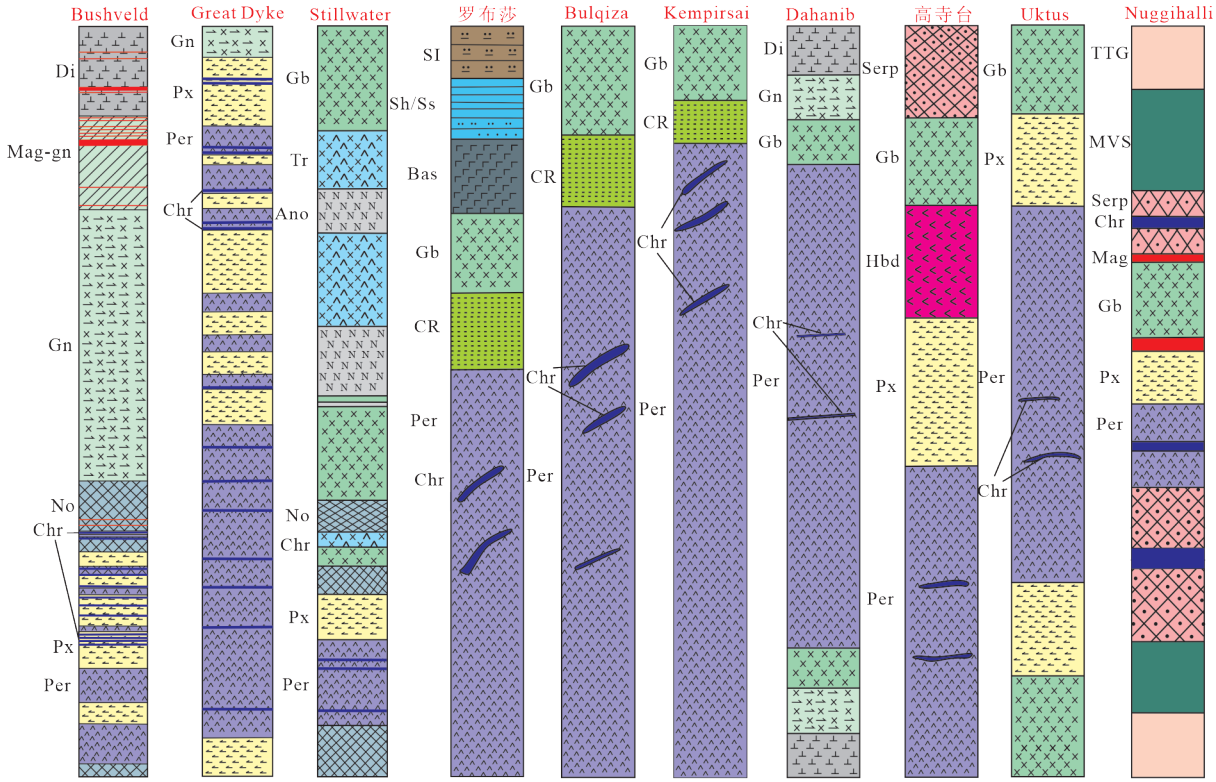
豆荚状铬铁矿则与造山带蛇绿岩套密切相关,其典型岩石组合自下而上分别为地幔橄榄岩、堆晶岩、辉长岩、席状岩墙群和枕状玄武岩(González-Jiménez et al.,2014a,2014b;Yang et al.,2021;Xiong et al.,2024)。这类矿体主要赋存于地幔橄榄岩中,尤其是上部高度亏损的方辉橄榄岩中(Nicolas and Azri,1990;González-Jiménez et al.,2014a),且常被纯橄岩薄壳所包裹(Zhou et al.,1996)。矿体受构造作用强烈控制,与剪切带存在密切联系,形态多呈透镜状、扁豆状或不规则状,同围岩呈截然或渐变接触(Page et al.,1984;González-Jiménez et al.,2014a,2014b)。相较于层状铬铁矿,豆荚状铬铁矿规模较小,分布较分散,但品位高。

阿拉斯加型铬铁矿产于与板块俯冲密切相关的

表 1　全球主要铬铁矿床矿体特征对比表

Table 1　Comparison of characteristics of orebodies in major chromitite deposits worldwide

矿床类型	矿床名称	岩体特征	矿体特征	赋矿岩性	资料来源
层状铬铁矿	Bushveld（南非）	漏斗状,外围有四个肢体,约65 000 km^2	层状产出,厚几十厘米至2 m	辉石岩、苏长岩	Eales et al.,1993,1996;Cawthorn et al.,2005
	Stillwater（美国）	顶部呈截断状的楔形体,约180 km^2	含十余条铬铁矿层,厚度从厘米级至8 m,储量约342万t	橄榄岩	McCallum,1996;Jackson, 1968;Cawthorn et al.,2005
	Great Dyke（津巴布韦）	呈向外延伸的堤坝形,长550 km,宽度范围为4~11 m	上部辉石岩中的铬铁矿层可厚达1.8 m,而下部超镁铁质部分多为10~20 cm	辉石岩、纯橄岩	Wilson,1996;Hamilton,1977;Cawthorn et al.,2005
	Kemi（芬兰）	最初为漏斗状,后倾斜成透镜状,长15 km,深部延伸超2 km	铬铁矿层主层为20 m,局部可达90 m,最薄至0.5 m	橄榄岩	Alapieti et al.,1989
	Ipueira-Medrado Sill（巴西）	岩床,长约7 km,厚约300 m	主铬铁矿层厚5~8 m,次生层厚0.3~1.1 m	方辉橄榄岩	Oliveira and Lafon,1995;Marques et al.,2003
豆荚状铬铁矿	Ray-IZ（俄罗斯）	新月状展布蛇绿岩体,出露面积约380 km^2	矿体以豆荚状、透镜状和脉状为主,部分呈巨厚层状	方辉橄榄岩、纯橄岩	Yang et al.,2015;Xiong et al.,2020a
	Guleman（土耳其）	不连续出露的蛇绿岩体,局部呈强烈蛇纹石化,局部存在累积-侵入组合	铬铁矿常呈透镜-豆荚状或层状	方辉橄榄岩、纯橄岩	Özkan et al.,1982;Sapanci et al.,2023
	Bulqiza（阿尔巴尼亚）	EasternMirdita蛇绿岩带中超基性岩体,面积约350~370 km^2	矿体主要为豆荚状、透镜状,少数为块状,部分为巨厚层	方辉橄榄岩、纯橄岩	Xiong et al.,2020a,2021;Qiu et al.,2019
	Oman（阿曼）	世界最大蛇绿岩体之一,面积约25 000 km^2	矿体多为透镜状、囊状	方辉橄榄岩、纯橄岩	Rollinson,2005;Borisova et al.,2012
	罗布莎（中国西藏）	位于雅鲁藏布缝合带南段,广泛发育蛇纹石化,出露宽约4~6 km,长约60 km	矿体多为透镜状、豆荚状	方辉橄榄岩、纯橄岩	Xu et al.,2009;Xiong et al.,2020a,2020b
阿拉斯加型铬铁矿	Kytlym（乌拉尔）	由多个小型透镜状、环状的超基性–基性岩体组成,规模较小、分布分散	铬铁岩常呈豆荚状体、异离体和细脉,少见块状透镜体和层状体,规模从数厘米至数分米不等	纯橄岩	Garuti et al.,2002,2003
	Nizhni Tagil（乌拉尔）	岩体呈环状/椭圆状,直径约8~10 km	铬铁矿体呈透镜状、豆荚状,单个矿体厚度1~5 m, 走向延伸几十至数百米	纯橄岩、异剥橄榄岩	Tessalina et al.,2015
	Uktus（乌拉尔）	多个小型的环状超基性-基性岩体复合而成,规模较小	铬铁岩常形成豆荚状体、异离体和细脉,少见块状透镜体和层状体,规模从数厘米至数分米不等	纯橄岩、异剥橄榄岩	Garuti et al.,2002,2003
	Kondyor（俄罗斯）	呈近乎完美的圆形,直径约6 km,面积约40 km^2	铬铁矿体以透镜体和脉体形式出现,大小不一,从数cm到约1.5m长、厚度可达15~20 cm	纯橄岩	Zhukova et al.,2025
	高寺台（中国）	呈近椭圆形,东西向延伸约9 km,中部最大宽度约1.5 km	铬铁矿体多呈透镜状、豆荚状,矿体厚度一般0.5~5 m,延伸几十米至上百米	纯橄岩	Yang et al.,2017;Xiong et al.,2023
绿岩带型铬铁矿	Ujaragssuit（格陵兰）	地表出露面积约800m×100 m,露头厚约50 m,具上、下两个岩浆旋回	层状、条带状(厚1~10 cm)和致密块状(最厚3 m)	纯橄岩	Rollinson et al.,2002;Nishio et al.,2025
	Nuasahi-Sukinda（印度）	Nuasahi出露长500~1000 m,宽300~450 m;Sukinda岩体规模约25 km×400 m	似层状、条带状、块状、网脉状等;发育滑塌构造、包卷结构	纯橄岩、斜方辉石岩、辉长岩	Mondal et al.,2006,2019
	Aladahalli（印度）	产于Nuggihalli绿岩带,绿岩带长约60 km,宽2 km	似层状或条带状,最大厚度约15 m,围岩受强烈剪切变形	蛇纹石化纯橄岩	Mukherjee et al.,2010,2012
	Railway Block（津巴布韦）	位于Selukwe超基性杂岩体内,受向斜和褶皱构造控制	似层状和透镜状,厚度几十米至几百米,沿走向断续延伸	(蛇纹石化)纯橄岩、斜方辉石岩	Prendergast,2008
	Black Thor（加拿大）	Bird River层状岩体的一部分,矿体延伸约600 m	厚层状,发育6条独立的铬铁矿层,总厚度约60 m	纯橄岩、辉长岩和辉石岩	Scoates and Jon Scoates,2013



资料来源同表1；Ano—斜长岩；Bas—玄武岩；Chr—铬铁矿；CR—堆晶岩；Di—闪长岩；Gb—辉长岩；Gn—辉长苏长岩；Hbd—角闪石岩；Mag—磁铁矿；Mag-gn—磁铁矿辉长苏长岩；MVS—变质火山岩片岩；No—苏长岩；Px—辉石岩；Per—橄榄岩；Serp—蛇纹岩；Sh—页岩；Ss—砂岩；Si—硅质岩；Tr—橄长岩；TTG—英云闪长岩-奥长花岗岩-花岗闪长岩岩石组合

图3 全球主要含铬铁矿岩体剖面对比图

Fig.3 Comparative cross sections of major chromitite-bearing complexes worldwide

镁铁-超镁铁质杂岩体中，岩体具典型的同心环带构造，平面上多呈环状、椭圆状或不规则状(表1；崔梦萌等，2020)，自中心向外依次为纯橄岩、异剥橄榄岩、单斜辉石岩、角闪石岩与正长辉长岩(Taylor，1967；Himmelberg et al.，1995)，且其中超基性岩与其外围辉长质岩接触界限截然不同。铬铁矿常呈条带状或准层状赋存于核部纯橄岩中，如Dahanib、高寺台和Uktus岩体，但绝大多数矿化均未达到可开采的规模(Irvine，1974；Himmelberg et al.，1995)。

绿岩带型铬铁矿主要分布于太古宙绿岩带中，围岩为低级或未变质的沉积-火山岩系(翟明国，2022)，主要岩石组合为玄武岩、科马提岩、中酸性钙碱质火山岩和沉积岩等，且多因蚀变或变质作用生成的绿泥石、绿帘石、阳起石等矿物而呈特征的暗绿色(Windley，1995；王嘉玮等，2023)。赋矿围岩以蛇纹石化纯橄岩为主，少数矿体产于辉长岩、斜长岩或方辉橄榄岩中，偶与含铁建造伴生，如印度Nuasahi Sukinda矿床(Saha，1994)。矿体产状复杂多样，包括层状或似层状与透镜状、不规则状三类，层状、似层状矿体规模通常较大，而透镜状、不规则状矿体规模较小(王嘉玮，2023)。矿体横向延伸不稳定，受后期构造变形影响明显，部分矿体沿走向断续延伸或与围岩呈大角度斜交，如津巴布韦Railway Block矿床(Tsomondo，1995)。

总的来说，四类铬铁矿均与超镁铁质岩存在紧密的时空与成因联系，但在赋矿岩石组合、矿体形态与规模上又表现出系统差异，反映出不同成矿体系中岩浆供给、储存方式与构造体制的不同，从而导致Cr元素富集路径的差异。

2 不同类型铬铁矿的矿物组合特征

矿石的矿物组合及其显微共生关系是成矿地质作用的直接记录，系统对比不同类型铬铁矿的矿物组合与PGE-硫化物赋存特征，可以约束成矿环境的物理化学条件，并为反演成矿流体组成与演化提供关键线索(González-Jiménez et al.，2014a，2014b；Robb，2020)。不同类型铬铁矿床的矿物组合见表2。

层状铬铁矿矿物组合以“铬尖晶石±橄榄石±斜方辉石±单斜辉石±斜长石”为主，少见金红石和钛铁矿，

表 2　全球主要铬铁矿床矿物组合对比表

Table 2　Comparison of mineral assemblages of major chromitite deposits worldwide

矿床类型	矿床名称	矿石矿物	脉石矿物	主要贱金属硫化物	次要贱金属硫化物	铂族矿物	参考文献
层铬铁矿	Bushveld（南非）	Chr, Ol, Plag, Opx, Cpx, Phl	Opx, Plag, Mic, Cpx, Ol	Po, Cp, Pn, Py	Gn, Cub, Sph	Lrt, Spe, Coo, Brg	Lee,1996;Schouwstra et al.,2000;Cawthorn et al.,2005;Voordouw et al.,2010
	Stillwater（美国）	Chr, Ol, Opx, Plag, Phl	Ol, Opx, Cpx, Plag	Po, Cp, Pn	Py, Mlr, Cub, Vi, Mo, Bn	Lrt, Mon, Spe, Coo, Brg, Vsk, Kot, Mer, Stw, Paa, Sbp	Talkington et al.,1986;Lee,1996;Cawthorn et al.,2005;Aird et al.,2017
	Great Dyke（津巴布韦）	Chr, Mgs, Tlc, Ol, Opx	Opx, Cpx, Ol, Plag	Po, Pn, Cp, Py	Gn, Bn	Spe, Ele, Brg, Coo, Lrt, Mon, Msl, Mich, Kot, Pol, Hgw	Lee,1996;Wilson,1996;Oberthür et al.,2003
	Kemi（加拿大）	Chr, Ol, Opx, Cpx, Amp, Plag	Ol, Opx, Cpx, Amp, Plag	Po, Pn, Cp	Gn, Sph	Lrt	Lee,1996;Sharkov et al.,1995
	BurakoVsky（俄罗斯）	Chr, Ol, Cpx, Opx, Plag, Phl, Amp	Ol	Py, Pn, Cp, Po	Cub, Mlr, Bn	Lrt, Erl, Mon, Mer, Fr, Kot, Spe, Brg, Mich, Ele, Gev, Mln, Pl, Hgw, Irs, Coo	Marques et al.,2003;Bailly et al.,2009
豆荚状铬铁矿	Kempirsai（哈萨克斯坦）	Chr, Ol, Cpx, Opx, Amp, Phl, Chl, Plag	Amp, Chl, Grt, Srp, Ilm, Ca-ti Ox	Mlr, Hzl	Cc, Py, Sph, Orc	Lrt, Erl, Rti, Bm-pge, Kash, Ru-os-ir al	Melcher et al.,1997;Yurichev et al.,2019;Saveliev et al.,2023
	Ray-IZ（俄罗斯）	Chr, Cpx, Opx, Ol, Plag, Chl	Cpx, Opx, srp, Chl, Mic, Plag, Qtz, Grt, Ky, Crn, Ap	Mlr, Orc, Py, Pn, Cp	Gn, Sph, Mo, Stb, Cv, Hzl, Nc	Lrt, erl, Os-ir al, Cir, Kash	Garuti et al.,1999;Yang et al.,2014;Xiong et al.,2020b
	Bulqiza（阿尔巴尼亚）	Chr, Ol, Opx, Cpx, Srp, Chl, Amp	Ol, Opx, Cpx, Srp, Chl, Amp, Di	Pn, Po, CPy	Mlr, Hzl, Py	Lrt, Erl, Os-ir al, Irs, Ras, Pt-Pd al, Spe	González-Jiménez et al.,2014a;Xiong et al.,2015,2021;Qiu et al.,2018
	Oman（阿曼）	Chr, Ol, Opx, Cpx, Srp, Chl, Amp, Di, Grt	Ol, Opx, Cpx, Srp, Chl, Amp, Grt	Pn, Po, Mlr, Cu-rich Ni-Fe-S	Gn, Hzl, Po, Cp	Lrt, Erl, Cir, Irs, Hgw, Ras, Paa, Spe, Osa, Ru-Os-Ir oxide	Augé et al.,1987;Lorand et al.,1989;Ahmed et al.,2002,2003;Arai et al.,2020
	罗布莎（中国西藏）	Chr, Ol, Opx, Cpx, Srp, Chl, Amp, Ph, Grt	Ol, Opx, Cpx, Srp, Chl, Amp, Phl, Mt, Grt, Di, Carb	Py, Pn, Po	Pn, Mlr, hzl, Sph, Gn, Tnt, Ttr, Cc, Spk	Lrt, Erl, Irs, Ras, Hgw, Spe	Zhou et al.,1996;Bai et al.,2000;Xiong et al.,2024
阿拉斯加型铬铁矿	Duke Island（阿拉斯加）	Chr, Ol, Cpx, Amp, Srp	Ol, Cpx, Amp, Srp	Pn, Po, CPy	CPy, Py		Irvine et al.,1974;Thakurta et al.,2008
	Kytlym（乌拉尔）	Chr, Ol, Cpx, Amp	Ol, Cpx, Amp, Phl, Chl, Tlc	Po, Pn	Py	Iso, Erl, Pt-Fe al, Coo, Tul, Pd-cu al, Ir-Fe al	Garuti et al.,2003;Zaccarini et al.,2013
	Uktus（乌拉尔）	Chr, Ol	Ol, Cpx, srp, Mt, Chl	Po, Pn	Hzl, Mlr	Iso, Erl, Pt-fe al, Coo, Lrt, Tul, Pd-Cu al, Ir-Fe al	Garuti et al.,2003;Zaccarini et al.,2018
	Kondyor（俄罗斯）	Chr, Ol, Mt, Cpx	Ol, Cpx, Phl, Chl, Srp, Amp	Po, CPy	Po	Iso, Pt-fe al, Lrt, Erl, Hgw, Spe, Pl, Tul, Hgs, Gev	Malitch et al.,2015,2020
	高寺台（中国）	Chr, Ol, Cpx, Mt	Grt, Cpx, Phl, Mgs, Ap	Py, Mlr	Gn	Lrt, Erl	Tian et al.,2011;Xiong et al.,2023
绿岩带型铬铁矿	Ujaragssuit（格陵兰）	Chr, Phl, Chl, Tlc, Ol	Phl, Chl, Tlc, Ol, Tr, Anth, Carb, Amp	Pn	Po, Cp	Ir, Os-ir al, Lrt, Erl, Ras, Irs	Rollison et al.,2002;Nishio et al.,2025
	Sukinda（印度）	Chr, Ol, Opx, Cpx	Tlc, Chl, Srp, Mgs, Kam, Uva	Po, Pn, Cp	Mlr	Lrt, Erl, Irs, Ras, Hgw, Ru-os-ir al	Chakraborty et al.,1984;Mondal et al.,2006,2019
	Railway Block（津巴布韦）	Chr, Ol	Chl, Tlc, Phl, Tr, Srp, Carb		Po, Pn, Cp	Lrt, Irs	Prendergast,2008;Cotterill,1969;Stowe,1994

注:Ac—辉银矿;Al—合金;Amp—角闪石;Anth—直闪石;Ap—磷灰石;Apy—毒砂;Ars—砷化物;Aw—自然镍铁合金;Bis—铋化物;Bm-Pge—基底金属-PGE合金;Bn—斑铜矿;Br—砷镍黄铁矿;Brg—硫铂镍矿;Bt—黑云母;Bta—硫铋铜矿;Carb—碳酸盐;Cat—硫钴矿;Cc—辉铜矿;Chl—绿泥石;Chrf—铁-铬合金;Cir—铜铱矿;Chr—铬铁矿;Coo—铜铂矿/硫化铂矿;Cp—黄铜矿;Cpv—铑砷硫矿;Cpx—单斜辉石;Crn—刚玉;Cr-Clc—含铬绿泥石;Cu-Sn—铜-锡合金;Cub—方铜矿;Cv—铜蓝;Di—透辉石;Dol—白云石;Ele—电子金;Erl—硫锇矿;Fr—弗鲁德矿;Gev—盖弗斯矿/铂锑矿;Gn—方铅矿;Goe—针铁矿;Grt—石榴子石;Hem—赤铁矿;Hgs—红石矿;Hgw—钌铑矿;Hzl—硫镍矿;I—铱砷矿;Ilm—钛铁矿;Irarsite—铱砷硫矿;Ir-Fe Al—铱-铁合金;Iso—铁铂矿;Kash—钌-铱-铑硫砷矿;Kln—高岭石;Kot—钯铂碲矿;Ky—蓝晶石;Lrt—硫钌矿;Lrs—铱砷硫矿;Mer—默氏矿;Mgs—菱镁矿;Mic—云母;Mich—镍铂碲矿;Ml—辉硫镍矿;Mln—马兰矿;Mlr—辉硫镍矿;Mo—辉钼矿;Moi—莫桑石;Mon—蒙氏矿;Msl—马斯洛夫矿;Mt—磁铁矿;Nc—红砷镍矿;Ngg—镍金矿;Ol—橄榄石;Ome—峨眉矿;Opx—斜方辉石;Orc—奥硫砷镍矿;Osa—锇砷硫矿;Os-Ir Al—锇-铱合金;Paa—砷钯矿;Pd—多硫镍矿;Phl—金云母;Pl—铂砷矿;Plag—斜长石;Pn—镍黄铁矿;Po—磁黄铁矿;Pol—极性矿;Pt-Fe Al—铂-铁合金;Pt-Pd Al—铂-钯合金;Py—黄铁矿;Qtz—石英;Ras—钌砷矿;Rt—金红石;Rti—钌-铱自然合金;Ru-Os-IrOx—钌-锇-铱氧化物;Sbp—锑钯矿;Ser—绢云母;Sie—锡根矿;Sig—锡根矿;Smc—蒙脱石;Smt—锑银矿;Sob—钯铋矿;Spe—砷铂矿;Sph—闪锌矿;Srp—蛇纹石;Stb—辉锑矿;Stw—斯蒂尔沃特矿;Sud—萨德伯里矿;Tfr—四铁白金矿;Tlc—滑石;Tlr—碲化物;Tnt—榍石;Tr—透闪石;Tul—图拉米恩矿;Txn—同心矿;Uva—铬钙榴石;Vi—紫硫镍矿;Vsk—维索茨克矿;Wc—曲松矿

其原生硅酸盐矿物常蚀变为蛇纹石、绿泥石和滑石，并常伴生磁铁矿、铬绿泥石、石榴子石、角闪石及方解石和白云石等碳酸盐蚀变相(Schulte et al.,2012)。硫化物常见磁黄铁矿、镍黄铁矿、黄铁矿、黄铜矿等，且多呈粒间充填或包裹体的形式产出。铂族矿物则以Pt-Fe合金、硫铂矿、铜铂矿、硫钌矿及Pt-Pd-Te/As相为主，通常出现在硫化物颗粒的边缘，仅月桂石(RuS_2)常以包裹体形式产于铬尖晶石(Molebale et al.,2011；O'Driscoll et al.,2016；Prichard et al.,2017)。不同层位中铬铁矿铂族矿物(PGM)组合存在较大的差异，如Bushveld岩体中UG2铬铁矿层底部含Pt硫化物、硫钌矿、Pt-Fe合金、Pt-Pd硫化物以及Pt-Rh-Cu硫化物，而中部与顶部则不含Pt-Rh-Cu硫化物，其前导层则更富集PGE-硫砷化物与PGE合金，记录了后期热液流体的改造过程(Peyerl,1982；Voordouw et al.,2010)。

豆荚状铬铁矿主要以"铬尖晶石+橄榄石±斜方辉石±单斜辉石"的矿石矿物组合为特征，且普遍遭受后期热液蚀变改造，伴生蛇纹石、绿泥石等次生矿物(Mosier et al.,2012；O'Driscoll et al.,2016)。该类型铬铁矿PGM较为稀少，以富集Os-Ir-Ru为特征，如Os-Ir-Ru合金、硫钌矿、硫锇矿等，而Pt、Pd矿物稀少(González-Jiménez et al.,2014a；O'Driscoll et al.,2016；Zaccarini et al.,2018)。PGM多以包裹体形式赋存于铬尖晶石内部，少见于铬铁矿裂隙或边部蚀变带中，且前者PGM自形程度较好，呈多边形，而后者多呈半自形至他形，常见筛孔状结构(O'Driscoll et al.,2016)。硫化物则以镍黄铁矿、磁黄铁矿和黄铜矿为主，且普遍出现镍铁合金、钯镍矿等金属互化物。值得注意的是，国内外多个蛇绿岩中的铬铁矿和地幔橄榄岩均发现了金刚石等超高压(UHP)和强还原矿物组合的存在(Yang et al.,2007,2015；Xu et al.,2009；2015；杨经绥等,2013；Das et al.,2015,2017；Tian et al.,2015；Huang et al.,2015；Lian et al.,2017；Wu et al.,2017；Xiong et al.,2016,2017,2020b,2024)，且这些异常矿物的结构及成分特征表明豆荚状铬铁矿可能形成于地幔深部，与壳幔循环过程密切相关(Robinson et al.,2015；Xiong et al.,2017；Dilek et al.,2018；徐向珍等,2018；Yang et al.,2021)。

阿拉斯加型铬铁矿的矿物组合则相对简单，典型组合为"铬尖晶石+橄榄石±单斜辉石±角闪石"，因普遍存在角闪石而明显区别于其他类型铬铁矿，指示其形成于富水的岩浆环境，可能与俯冲流体或地壳混染有关(Himmelberg and Loney,1995；El-Rahman et al.,2012；Abdallah et al.,2019)。此外，阿拉斯加型铬铁矿PGM组合单一，以富Pt矿物为主，而富Os-Ir-Ru相对稀少。其中Pt-Fe-Ni-Cu体系的合金最为丰富，包括铁铂矿、四铁白金矿、图拉米恩矿(Pt_2FeCu)以及少见的含Fe或Fe+Ni自然铂以及红石矿(PtCu)，且常与硫钌矿-硫锇矿固溶体系列共生(Garuti et al.,2003；Nekrasov et al.,2005；O'Driscoll et al.,2016)。硫化物以磁黄铁矿、黄铜矿和镍黄铁矿为主，整体反映出富水-高氧逸度而硫不饱和的成矿环境。

相较于前三类铬铁矿，绿岩带型铬铁矿受后期蚀变作用影响更为强烈，且不同绿岩带产出的铬铁矿矿物组合基本相同，主要为"铬尖晶石+富镁橄榄石+斜方辉石±单斜辉石±角闪石±金云母"，常见堆晶橄榄石充填粒间间隙而呈韵律堆晶结构。此外，由于后期低级变质作用的影响，Fe^{2+}和Fe^{3+}常置换铬尖晶石结构中的Mg^{2+}和Al^{3+}，从而形成中心部分富镁，边部为富铁的核边结构(Evans and Frost,1975；González-Jiménez et al.,2009)。硫化物在绿岩带型铬铁矿中并不常见，仅少量以粒间充填或裂隙充填形式产出，主要类型为针硫镍矿、磁黄铁矿与黄铜矿等；与豆荚状铬铁矿类似，其PGM组合同样以IPGE为主导，包括富Os-Ir-Ru的合金、硫钌矿、硫砷铱矿等，但粒度更细(多小于5 μm)、热液-变质叠加现象更明显，常出现砷铂矿、砷硫铱矿等富As相，指示绿片岩相变质-流体阶段PGE的再活化与局部富集(O'Driscoll et al.,2016)。

整体来看，层状铬铁矿中硅酸盐矿物组合相对复杂，硫化物较发育并伴生富Pt-Pd型PGM；豆荚状和绿岩带型铬铁矿则以铬尖晶石+富镁橄榄石为主，PGM粒度细小，以富Os-Ir-Ru相为主，硫化物含量普通较低；而阿拉斯加型铬铁矿广泛发育角闪石和富Pt合金；四类铬铁矿在硅酸盐矿物、PGM和硫化物组合上的系统差异，反映了不同构造环境和物理化学条件下铬铁矿成矿过程的多样性。

3 铬铁矿矿床中矿物地球化学和全岩PGE特征

3.1 铬尖晶石成分特征

本文系统收集了来自15个不同类型铬铁矿体中2600余个铬尖晶石成分数据，并结合Barnes和Roeder(2001)数据库中铬尖晶石分析结果进行综合对比与归纳。结果表明，不同类型铬铁矿的铬尖晶石成分表现出显著差异，反映其成矿岩浆来源、部分熔融程度及后期演化过程存在明显不同。

层状铬铁矿床中的铬尖晶石普遍具有偏高的$Cr^{\#}$(56.00~78.75)和中等的$Mg^{\#}$(23.63~69.37)，其中以Great Dyke的$Cr^{\#}$最高(71.26~78.45)，Bushveld的$Mg^{\#}$最低(23.5~46.1)。在该类铬铁矿床中，随着$Cr^{\#}$的降

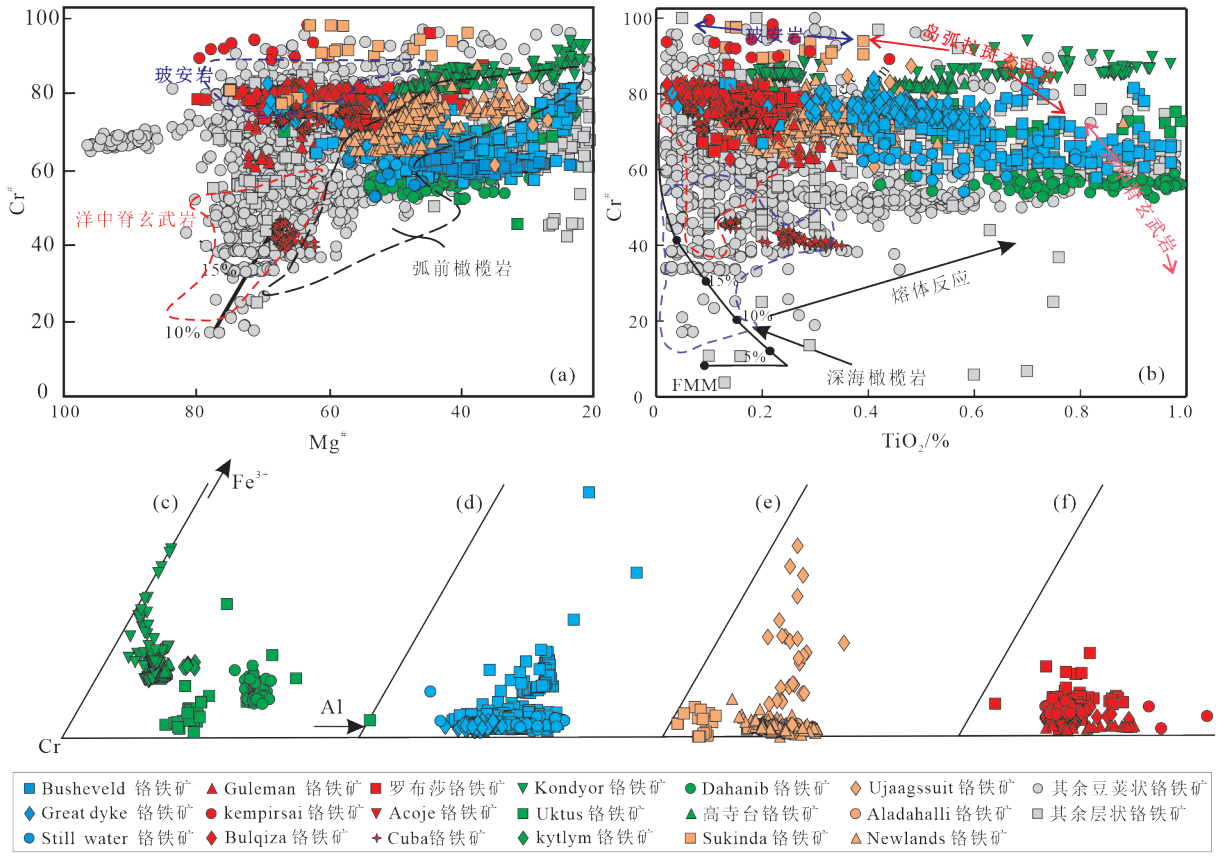
低,$Mg^{\#}$也随之下降,而TiO_2含量则呈显著升高趋势(图4a、4b),指示在稳定的岩浆房环境中,随橄榄石、辉石等矿物的持续结晶,残余熔体中Mg^{2+}活度降低与Cr不断消耗的岩浆分异过程(Irvine,1977;Hulbert and Von Gruenewaldt,1985)。

豆荚状铬铁矿中铬尖晶石的$Cr^{\#}$与$Mg^{\#}$变化范围极大,而TiO_2含量相对偏低,其中Kempirsai铬铁矿表现出异于典型豆荚状铬铁矿的特征,其$Cr^{\#}$异常高且落于玻安岩区域之外,推测其源于极端熔融,高度亏损的地幔源区(Melcher et al.,1997)。该类型铬铁矿成分极为复杂(图4a、4b),既存在单成因类型——MOR型或SSZ型(Gamal El Dien et al.,2019;谢慧丹等,2025),也存在兼具MOR和SSZ特征的多成因型(Qiu et al.,2019;Xiong et al.,2020b,2021,2024;Xu et al.,2023),反映出豆荚状铬铁矿成矿环境的多样性以及成因机制的多阶段特征。

而阿拉斯加型铬铁矿中铬尖晶石的$Cr^{\#}$与$Mg^{\#}$整体呈弱正相关关系,而$Cr^{\#}$与TiO_2则呈弱负相关,但该趋势并不稳定,局部存在明显偏离主趋势的样品点,如Kondyor铬铁矿中部分铬尖晶石在较低$Mg^{\#}$条件下仍表现出异常高的$Cr^{\#}$(可达90),表明$Cr^{\#}$与$Mg^{\#}$在个别样品中发生解耦。不同岩体中铬铁矿的成分表现出显著的分层性,高寺台和Kondyor铬铁矿$Cr^{\#}$相对较高(>80),Uktus铬铁矿的$Cr^{\#}$处于中等范围(60~80),而Dahanib铬铁矿的$Cr^{\#}$相对较低(<60),但均落入弧前地幔橄榄岩区域,反映出弧下地幔源区的不均一性。

绿岩带型铬铁矿中铬尖晶石普遍具有较高的$Cr^{\#}$(>60)和中等偏高的$Mg^{\#}$(26.70~75.06),二者呈负相关。其TiO_2含量变化较大,部分矿床如澳大利亚Newlands的TiO_2含量较高(0.33%~0.47%),而格陵兰Ujaragssuit和印度Sukinda的TiO_2含量较低,表明不同绿岩带内的铬铁矿床可能起源于不同的构造环境。

在Cr-Al-Fe^{3+}图解中,层状铬铁矿、豆荚状铬铁矿和绿岩带型铬铁矿中的铬尖晶石普遍集中于Cr-Al一带,而Fe^{3+}含量相对较低(图4d~4f)。个别矿床呈现特殊的成分特征,如Ujaagssuit绿岩型铬铁矿和Bushveld



数据来源:Garuti等(2003);Zaccarini等(2011);Lenaz等(2012);Barnes和Jones(2013);Uysal等(2018);Mondal等(2019);孙凯等(2019);Khedr 等(2020);Langa等(2021);Xiong等(2023,2025);赵金召等(2025);Zhukova等(2025)

图4 全球主要铬铁矿矿床中铬尖晶石成分图解

Fig.4 Diagrams for compositions of chromian spinels from major chromitite deposits in the world

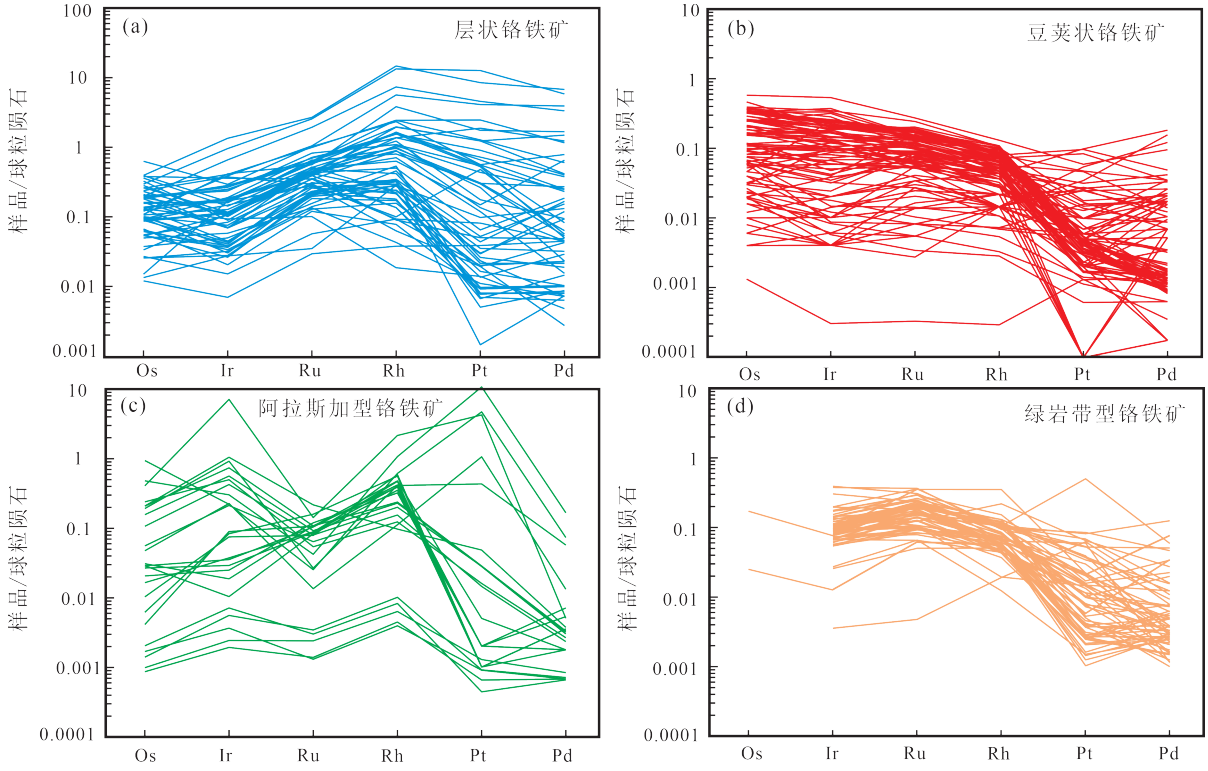
铬铁矿尖晶石的Cr/Al值相对恒定，而Fe^{3+}逐渐增加（图4d、4e），揭示了早期富铬熔体经历分异后，铬铁矿与残余熔体之间发生的再平衡过程（Rollinson et al.，2002）。阿拉斯加型铬铁矿中的铬铁尖晶石则表现出Fe^{3+}和Al富集的两大趋势（图4c），其中Fe^{3+}富集趋势可能与高氧逸度条件下铬铁矿与晶间流体的反应有关（Barnes and Roeder，2001；Krause et al.，2007）。而Al富集趋被认为形成于高压环境（Irvine，1967），或其成分受分异岩浆中缺乏含铝矿物相的缓冲作用影响（Sigurdsson and Schilling，1976）。

总体来看，四类铬铁矿床中铬尖晶石的成分特征存在系统差异：层状和绿岩带型整体表现为高$Cr^{\#}$、中等偏高$Mg^{\#}$，豆荚状型成分跨度最大，而阿拉斯加型则集中于弧前地幔橄榄岩域并表现出$Cr^{\#}$与$Mg^{\#}$的弱正相关关系，个别矿体存在局部解耦现象。在Cr-Al-Fe^{3+}图解中，层状、豆荚状及绿岩带型多沿Cr-Al轴分布，而阿拉斯加型则发育Fe^{3+}富集和Al富集两类演化趋势，反映出不同类型铬铁矿的成矿岩浆体系在氧逸度、压力条件及源区性质上存在显著差别。

3.2 铬铁矿的铂族元素组成特征

铂族元素（PGE）根据相容性差异，可分为IPGE（Os，Ir，Ru）和PPGE（Rh，Pt，Pd），其分布特征可有效指示部分熔融程度、硫逸度、地幔交代作用及熔岩反应等，是基性-超基性岩浆演化灵敏的指示剂（Barnes et al.，1985；Zhou et al.，1996；Grammatikopoulos et al.，2011）。

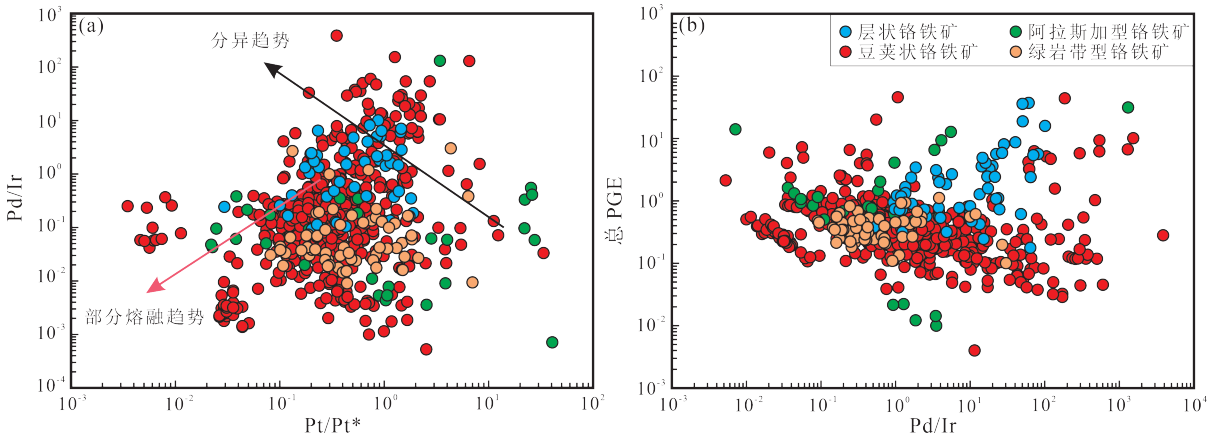
层状铬铁矿整体富集PPGE，相对亏损IPGE，呈铂族元素球粒陨石标准化曲线呈左倾型（图5a），∑PGE含量较高，可达数百至数千ppb，Pd/Ir>1，指示强烈的硫化物熔离和PPGE富集作用。此外，少数层状铬铁矿床（如Stillwater矿床）中的铬铁矿层IPGE+Rh特别富集，而Pt、Pd相对亏损，揭示了硫化物饱和历史及脱硫作用在PGE再分配过程的控制作用（Barnes et al.，2016）。豆荚状铬铁矿∑PGE含量变化极大，从极贫（$<100\times10^{-9}$）到高度富集（$>1000\times10^{-9}$）均有，其铂族元素球粒陨石标准化配分型式与绿岩带型铬铁矿类似（图5b、5d），整体以富集IPGE，亏损PPGE为显著特征，常被解释为高度亏损的地幔橄榄岩与硫不饱和熔体发生反应的结果（Zhou et al.，1998；Ahmed et al.，2002；Büchl et al.，2004；Zaccarini et al.，2024）；阿拉斯加型铬铁矿铂族元素配分图可见显著的Ir、Pt正异常与Ru、Pd的负异常，从而呈特征的“M”型配分型式，反映了弧



球粒陨石数据据Anders和Grevesse（1989）；数据来源：Rollinson等（2002）；Garuti等（2003）；Zaccarini等（2011）；Barnes和Jones（2013）；Uysal等（2018）；Mondal等（2019）；Zaccarini等（2024）；Xiong等（2023，2025）；Zhukova等（2025）

图5 不同类型铬铁矿中铂族元素球粒陨石标准化配分模式图

Fig.5 Chondrite-normalized distribution patterns of platinum-group elements (PGE) for chromitite samples from different types of chromitite deposits



数据来源同图5

图6 不同类型铬铁矿铂族元素二元图解

Fig.6 Binary diagrams for compositions of platinum-group elements (PGE) of chromitites from different types of chromitite deposits

前高镁岩浆在特定氧逸度和硫逸度条件下,PGE在金属/硫化物、铬尖晶石和熔体之间发生强烈分馏和多阶段结晶-再分配(Amossé et al.,2000;Garuti et al.,2003;O'Driscoll et al.,2016;Zaccarini et al.,2018)。此外,在Pt/Pt*-Pd/Ir图和∑PGE-Pd/Ir图中(图6a、6b),层状铬铁矿整体Pd/Ir偏高,且常随Pt/Pt*升高而下降,指示其PGE组分受演化岩浆-硫化物体系多阶段分馏过程控制;豆荚状铬铁矿多落在低Pd/Ir、低至中等Pt/Pt*区域,沿部分熔融趋势线分布,体现典型地幔残余属性;绿岩带型多处于中间带,反映残余与分异过程的叠加与再平衡;而阿拉斯加型分散度较大,既有低Pd/Ir的残余特征点,也有受分异影响而Pd/Ir偏高的样品,且表现出∑PGE与Pd/Ir的显著解耦。

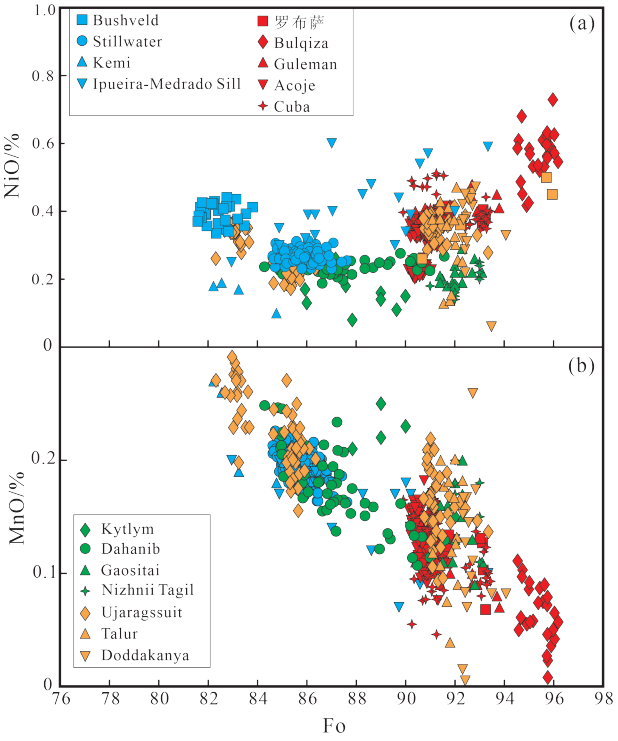
3.3 脉石矿物橄榄石成分特征

在橄榄石-熔体体系中,Ni为高度相容元素,其分配系数受熔体中MgO含量影响(Hart and Davis,1978;Li and Ripley,2010),在岩浆分异过程中与Mg表现出相似的地球化学行为,优先进入早期结晶的橄榄石;相反,Mn在橄榄石中为不相容至弱相容元素,更易滞留于演化熔体并进入晚期结晶相(Hart and Davis,1978;Klock and Palme,1988)。因此,橄榄石的Fo值及其NiO、MnO含量和相关性对岩浆分异过程及部分熔融程度具有重要指示意义(Ammannati et al.,2016)。

在橄榄石Fo-NiO和Fo-MnO图解中(图7a、7b),层状铬铁矿寄主橄榄岩中橄榄石Fo普遍集中于78~88,NiO含量变化范围较窄,且随着Fo值的升高,MnO含量降低,而NiO含量升高,显示出典型的原始镁铁质岩浆堆晶成因特征(De Hoog et al.,2010;Wang et al.,2021)。其中Ipueira-Medrado岩床中寄主橄榄岩的NiO值表现出相对分散的特征,被认为与多期高镁岩浆补给及局部硫化物矿化作用有关(Marques et al.,2003);而Stillwater橄榄岩中橄榄石局部呈轻微的NiO与Fo的负相关关系,被解释为橄榄石与硫化物熔体相互作用的结果(Barnes and Naldrett,1985)。相比之下,豆荚状铬铁矿寄主橄榄岩中橄榄石普遍呈现高镁特征(Fo>90),NiO中等偏高且变化范围较大,而MnO含量普遍偏低。同时,随着Fo值的升高,NiO含量升高,而MnO含量显著降低,指示强烈的部分熔融及熔体抽离作用(De Hoog et al.,2010;Su et al.,2019;Chen et al.,2020)。

阿拉斯加型铬铁矿的寄主橄榄岩中橄榄石整体呈现富镁特征,Fo值相对较高(82~93),但Ni含量相对偏低(Bai et al.,2017;Abdallah et al.,2019)。此外,NiO与Fo整体呈弱正相关,而MnO与Fo普遍呈负相关,反映了弧前高镁、富水母岩浆在通道化结晶分异过程中,基底金属硫化物与铂族合金的早期分离及其与共生铬尖晶石之间的Fe-Mg交换过程(Krause et al.,2007;Bai et al.,2017;Abdallah et al.,2019)。绿岩带型铬铁矿寄主橄榄岩的橄榄石成分与豆荚状类型相似,同样表现出高Fo、高NiO、低MnO的特征,但随着Fo值的升高,NiO略微增高,而MnO则急剧下降,指示绿岩带型橄榄岩经历了更为极端的高程度部分熔融和持续的熔体抽离过程。值得注意的是,Ujaragssuit铬铁矿部分样品Fo值相对较低,且随着Fo升高,NiO和MnO均呈下降的趋势,可能记录了局部晚期熔体-岩石反应或相对富集岩浆的交代作用(Rollinson et al.,2002;Sawada et al.,2023;Nishio et al.,2025)。

由上述对比可知,层状铬铁矿的寄主橄榄岩中橄榄石多具有中等偏高Fo值和NiO含量,变化范围较窄且MnO随Fo升高而降低,符合原始镁铁质岩浆堆晶橄榄石



数据来源：Marques等(2003)；Tian等(2011)；Zaccarini等(2011)；Jenkins等(2018)；Veksler等(2018)；Khedr等(2020)；Zhang等(2020)；Rui等(2022)；Rizeli等(2023)；Xiong等(2023)；Hayes等(2025)；Xiong等(2025)

图7 不同类型铬铁矿寄主橄榄岩中橄榄石成分图解

Fig.7 Diagrams for compositions of olivines in host peridotites of different types of chromitite deposits

的常见特征。豆荚状和绿岩带型铬铁矿寄主橄榄石整体具有更高的Fo和NiO、较低的MnO，且NiO随Fo升高而增加、MnO显著降低的趋势更为突出，大体与较高程度部分熔融及持续熔体抽离背景相吻合。阿拉斯加型铬铁矿寄主橄榄石则兼具较高Fo和相对较低NiO，并表现出NiO和Fo呈弱正相关、MnO和Fo呈负相关的组合。

4 不同类型铬铁矿的成因模式

4.1 层状铬铁矿成因

如前所述，层状铬铁矿的矿体产状、铬尖晶石及围岩橄榄石的成分均呈现出岩浆分异的典型特征(图4、7)，因此传统观点认为层状铬铁矿是由母岩浆结晶分异形成铬尖晶石，并在重力作用下沉降堆积于岩浆房底部形成的(Irvine，1975；Cameron，1980；Cawthorn，2005)。然而，成矿母岩浆的原始Cr含量(通常小于0.35%)不足以支撑层状侵入体中致密至半致密铬铁矿层(常达1 m，少数可达10 m，个别甚至可达100 m)的形成(表1)(Eales，2000；Cawthorn et al.，2005)。基于这一核心矛盾，层状铬铁矿的成因机制研究长期聚焦于Cr的富集机制及其堆积成层过程。

关于层状铬铁矿中Cr的富集机制，Irvine(1975，1977)提出原始富镁玄武质岩浆与演化岩浆之间的混合可使熔体成分跨越相平衡边界，从而在短时间内诱发铬尖晶石的集中结晶，这也是现今最为广泛接受的主流观点。与此同时，实验岩石学研究指出，铬尖晶石的稳定域对温度、氧逸度及熔体组成极为敏感，适度的ΔT或Δf_{O_2}变化可显著降低熔体中Cr的溶解度，从而触发铬尖晶石的大量结晶(Murck and Campbell，1986；Ulmer，1969；Ferreira Filho and Araujo，2009)。在此基础上，部分学者强调围岩同化混染在调控熔体成分与氧逸度中的作用，尤其是Stillwater杂岩体中铬铁矿所含的熔体包裹体和多相包裹体被认为是原始岩浆在顶板停滞并发生同化混染的直接证据(Spandler et al.，2005)。近年来，压力效应重新受到关注，Latypov等(2018)通过相平衡拓扑分析和热力学模拟提出，深部玄武质熔体在上升减压过程中可能进入铬尖晶石单相饱和域，随后在浅部岩浆房中结晶形成厚层铬铁矿。此外，基于特定铬铁矿层或特定矿床现象的研究，前人提出了诸如液态不混溶(McDonald，1965)、同化富Fe建造(Rollinson，1997)、富水或外来流体加入(Prendergast，2008；Azar，2010)等成因模型。

关于铬铁矿层的形成位置及成层方式的争议更为集中，传统观点认为铬铁矿层是在岩浆房底部堆积形成(Irvine，1975；Cameron，1980；Cawthorn，2005；Spandler et al.，2005)。然而，该模型并无法解释铬铁矿层似岩床侵入的产状、铬尖晶石与硅酸盐矿物呈现高度均一的镶嵌结构、铬铁矿与围岩之间的反应边界等现象，并由此提出了致密铬铁矿并非形成于岩浆房底部，而是形成于堆晶层序的深部，且不涉及仅铬尖晶石饱和的岩浆。Naldrett(2012)总结并将其划分为原位结晶和异位结晶-运移两大类(图8)。异位结晶-运移包括两大模型：(1)先期岩浆房中铬尖晶石和斜方辉石共结晶，随后在注入层状侵入体相关岩浆房的过程中被分选出来，最终以铬铁矿富集浆体的形式在堆晶体-岩浆界面上成层分布(Eales，2000；Mondal and Mathez，2007；Voordouw et al.，2009)(图8a)；(2)早期层状侵入体的规模远大于现今所见，在后期地壳负荷作用下岩体中心逐渐下沉，部分固结的铬铁矿层被重新活化并向下滑移，从而使现今所保存的残余铬铁矿层加厚(Cameron，1980)(图8b)。而原位结晶则强调由于局部物理化学条件的改变(如氧逸度、压力或岩浆混合等)使铬尖晶石成为唯一或主要液相线矿物，从岩浆中直接、就地大量结晶堆积形成(Ulmer，1969；Irvine，1975，1977；Cameron，1980；Lipin，1993；Cawthorn et al.，2005)(图8c)。

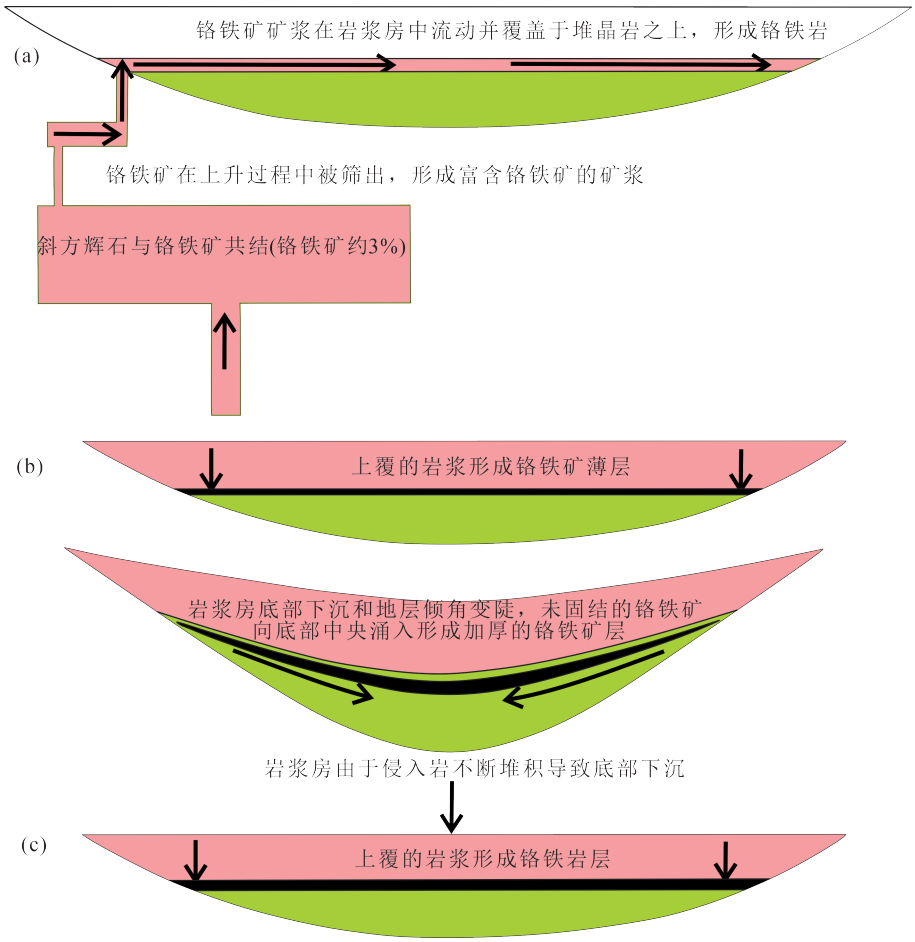


图8 层状铬铁矿形成模式(据Naldrett et al.,2012修编)

Fig.8 A model for the formation of layered chromitite deposit (modified after Naldrett et al.,2012)

4.2 豆荚状铬铁矿成因

豆荚状铬铁矿的成因机制长期存在较大的争议,早期的研究认为豆荚状铬铁矿的形成与层状铬铁矿类似,是由岩浆房中的基性-超基性岩浆通过分离结晶形成(Thayer,1964;Dickey,1975;Greenbaum,1977;Paktunc,1990)。随后为了解释残余地幔中铬铁矿的形成,又提出了形成于早期过渡带或深部岩浆房中的铬铁矿,经构造变形或重力沉降下移并进入残余地幔顶部的观点(Dickey,1975;Greenbaum,1977)。但该模型并无法解释豆荚状铬铁矿在产状、结构和共生矿物组合上与层状铬铁矿的系统性差异(Zhou et al.,2014;Latypov et al.,2017)。而后,前人基于对地幔橄榄岩的深入研究,发现豆荚状铬铁矿多赋存于高度亏损的方辉橄榄岩和纯橄岩中,且随着部分熔融程度的升高,铬尖晶石由富铝型逐渐过渡为富铬型,进而提出熔融残余成因模型(Lago et al.,1982;Duke,1982;Nicolas,1983)。但单纯依靠地幔橄榄岩的高度部分熔融,无论在质量平衡还是物理条件上,都无法合理解释矿床级Cr储量的形成(Kelemen et al.,1995;Zhou et al.,2014;陈艳虹等,2018)。

随着对蛇绿岩研究的不断深入,研究者发现豆荚状铬铁矿围岩的纯橄岩和方辉橄榄岩稀土元素配分模式呈现不同于现代橄榄岩的“U型”,被认为是俯冲带上的流体或熔体与残留橄榄岩反应的结果,由此提出熔岩反应成矿模型(Zhou et al.,1994,1996,1998;Arai,1997;González-Jiménez et al.,2014a,2014b),并认为板块俯冲消减带上残存的亏损方辉橄榄岩与玻安质或玄武质熔体发生反应而分别形成高铬型铬铁矿和高铝型铬铁矿(Zhou et al.,1994)。原位Re-Os同位素研究表明,铬铁矿的成矿物质不仅来自对流上地幔,还可能存在超大陆岩石圈地幔的贡献,于是在熔岩反应模型基础上提出熔体-古大陆岩石圈地幔混合成矿模型(Shi et al.,2007,2012),此模型强调古老岩石圈再循环对成矿的重要性。此外,非传统稳定同位素(Fe、Mg、Cr、Li等)揭示了富水流体在铬铁矿形成中的关键作用,认为橄榄石因亲熔体相而分离,同时亲流体相的铬尖晶石微晶通过吸附流体形成低密度不混溶液滴,且在岩浆运移中不断汇聚长大,并最终从边部至核

部结晶同时捕获并圈闭矿物包裹体形成铬铁矿(苏本勋等,2018,2021)。

上述有关豆荚状铬铁矿的成矿模型都局限于浅部岩石圈地幔环境。然而,随着蛇绿岩地幔橄榄岩和铬铁矿中金刚石等超高压矿物,以及一系列强还原矿物组合的发现,如呈斯石英假象的柯石英(Yang et al.,2007)、柯石英-单斜辉石出溶组合指示的CF型超高压结构的多型矿物退变产物(Yamamoto et al.,2009)、青松矿(Dobrzhinetskaya et al.,2014)、金红石的高压相多型(Xiong et al.,2024)等,向传统低压成因假说提出了质疑。在此背景下,学者们围绕豆荚状铬铁矿的成因机制提出了一系列新的成矿模型,包括俯冲板片混染模型(Shi et al.,2012;Zhou et al.,2014;Robinson et al.,2015;Arai and Miura,2016)、深俯冲-快速折返模型(Arai,2013; Griffin et al.,2016a)、微粒金刚石低压C-O-H流体成因模型(Farré-de-Pablo et al.,2019)、闪电击穿-等离子体凝结模型(Ballhaus et al.,2017,2021)、地震诱发瞬变高压变质模型(Huang et al.,2014;Griffin et al.,2016b;Yang et al.,2017)、陨石撞击成矿模型(Su,2022;Su et al.,2025)等。需要指出的是,上述模型多从构造位置、物理过程或瞬变压力-温度条件出发,对金刚石、青松矿、Fe-Ti合金以及高压多型金红石等异常矿物的成分组成和矿物组合缺乏系统的制约。相较之下,深成起源模型(Robinson et al.,2004;Yang et al.,2014,2021;Das et al.,2017)基于金刚石的成分特征认为俯冲将再循环岩石圈地输送至地幔过渡带乃至下地幔,而后经脱水与部分熔融形成流体与熔体。其中含碳流体在约150 km至下地幔不同深度结晶形成金刚石,蛇绿岩中的金刚石即来源于俯冲流体中的有机碳并在不同深度被铬铁矿包裹;最终,含金刚石铬铁矿随地幔对流上升,在洋中脊或俯冲带上方聚集形成透镜状铬铁矿体(图9)。此外,Xiong等(2015,2020,2024)基于异常矿物的成分与组合特征,将豆荚状铬铁矿的成因进一步划分为地幔深部地幔柱和地幔对流、大洋岩石圈中地幔橄榄岩部分熔融与岩浆分异、俯冲带岩石熔体反应以及晚期热液蚀变等四个阶段。

4.3 阿拉斯加型铬铁矿成因

关于阿拉斯加型铬铁矿的成因,目前普遍认为与俯冲带相关的岛弧-弧前环境中富水基性-超基性岩浆的结晶与演化过程密切相关,但具体成因机制仍存在较大争议。一类模型强调弧下或弧根部岩浆房的分离结晶与重力堆积,认为高Mg、富水、较高f_{O_2}的弧前岩浆在深部或浅部岩浆库内发生强烈分异与岩浆混合,在局部达到Cr饱和后优先结晶铬尖晶石,并形成层状、带状或透镜状铬铁矿体(Irvine,1967;Himmelberg and Loney,1995;Garuti et al.,2012;Wang et al.,2023)。而另一类模型则强调通道化高镁岩浆在纯橄岩通道及其膨大空腔中的动态富集作用,即持续供给的高温岩浆在狭窄上升通道与局部膨大部位产生对流与剪切,

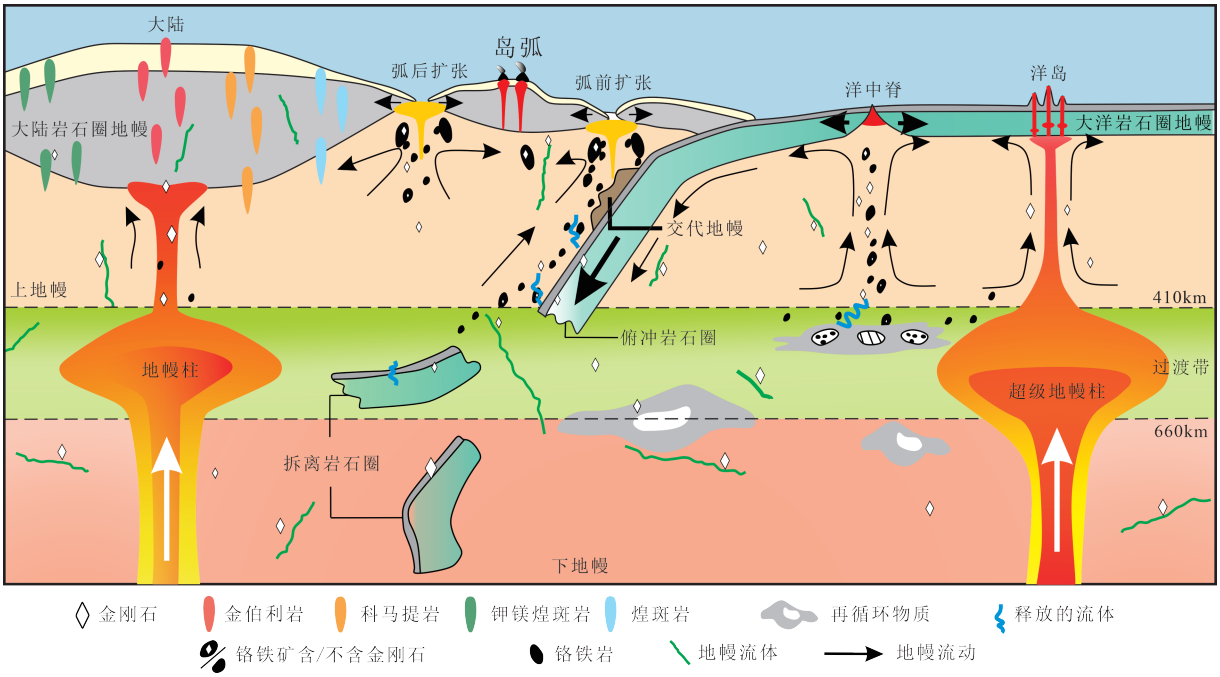


图9 豆荚状铬铁矿的深成起源模型(据Yang et al.,2021修编)

Fig.9 A model for the formation of deep mantle originated podiform chromitite deposit (modified after Yang et al.,2021)

促使铬尖晶石与富Pt的PGE合金协同富集,形成沿通道分布的条带状、脉状铬铁矿(Lago et al.,1982;Augé,2005;O'Driscoll et al.,2016)。此外,对乌拉尔-阿拉斯加型杂岩体的系统研究表明,同生堆晶铬铁矿与后期熔体-流体交代形成的脉状、网脉状铬铁矿往往共存,记录了从早期岩浆堆晶到晚期富水熔体/流体改造的多阶段成矿过程(Garuti et al.,2012;Zaccarini et al.,2018)。

在上述背景下,埃及东部沙漠Dahanib阿拉斯加型复合体为弧下深部岩浆-通道系统中带状铬铁矿的成因提供了关键约束。Khedr等(2020)认为,俯冲板片释放的富水流体交代地幔楔并诱发部分熔融,产生富水、高Mg的弧前高镁岩浆,并沿近似柱状的纯橄岩通道向上运移。岩浆在狭窄上升通道及其局部膨大部位发生反复脉动和通道化流动,使局部熔体达到Cr饱和,富Cr的铬尖晶石优先结晶并在纯橄岩通道及其扩张空腔中发生动力学富集,形成条带状、层状铬铁矿层;随后持续的岩浆补给以及晶浆重力滑移与再堆积,进一步促使铬铁矿在管道核部进一步集中,并与晚期从残余熔体中分离的富PGE硫化物共同组成Cr-Ni-Cu-PGE成矿系统(图10)。

4.4　绿岩带型铬铁矿成因

目前针对太古宙绿岩带铬铁矿成矿相关的岩浆过程及成矿物质富集机制的研究仍相对匮乏。早期的研究认为,绿岩带型铬铁矿形成于基性-超基性的岩浆分离结晶作用,由开放岩浆系统内科马提质岩浆或高Mg玄武质岩浆经过火成堆积作用或结晶分异作用形成(Mondal and Mathez,2007;Prendergast,2008;Scoates and Jon Scoates,2013)。但要形成1 m厚的铬铁矿层,大约需要数千倍同体积的科马提岩岩浆(Cawthorn et al.,2005),这一结果对单一分离结晶模型提出了挑战。此后,绿岩带型铬铁矿的成因研究多沿用前文层状侵入体致密铬铁矿层所建立的成矿机制,包括分离结晶、岩浆混合、堆晶-熔体反应和同化铁建造等,但这些模型也均未能很好地解释巨厚铬铁矿层的物质来源和质量平衡不足的核心问题。基于此,Lesher等(2019)提出Fe-Ti氧化物转化为铬铁矿的成因模型,并以此解释Black Thor铬铁矿中巨厚铬铁矿层的形成,其核心机制可概括为三个阶段:(1)动态岩浆通道环境中,富Fe±Ti氧化物岩石(如氧化相铁建造或富铁辉长岩)发生部分熔融,可熔性硅酸盐组分被科马提质岩浆同化吸收,而细粒磁铁矿、钛铁矿等不溶性氧化物则以捕掳晶形式被卷入通道化上涌的富Cr岩浆中;(2)在高岩浆/氧化物质量比的条件下,岩浆中的Cr、Al等元素向氧化物颗粒中扩散迁移,同时氧化物中的Ti元素向岩浆中释放,促使原始Fe-Ti氧化物在短至数天的时间内逐步转化为富Cr的铬铁矿;(3)新生成的高密度铬铁矿晶体,在流经岩浆通道的膨大部位或流速减缓区域发生物理富集与堆积,最终形成厚度可达数十米乃至更大规模的致密-半致密铬铁矿层(图11)。

5　全球不同类型铬铁矿成矿与地球演化过程

为系统研究不同类型铬铁矿的时空分布特征,本文基于前人研究共计汇总了1192个铬铁矿床的年龄及赋存岩体规模,结果显示显著的分段性特征(表3,图12a)(Mosier et al.,2012;Thakurta,2018;Arai et al.,2018;Smith et al.,2021)。其中,绿岩带型铬铁矿主要集中分布于太古宙;层状铬铁矿分布时限较长,为太古宙-古元古代;阿拉斯加型和豆荚状铬铁矿则多产出于古生代-中生代,仅见有极少数太古宙豆荚状铬铁矿的记录,这与前人研究基本一致(Stowe et al.,1994;Arai

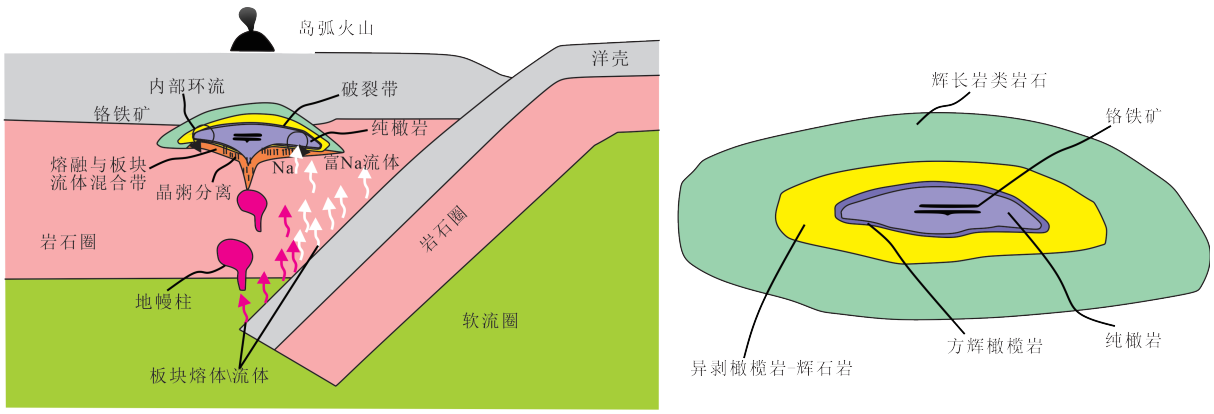
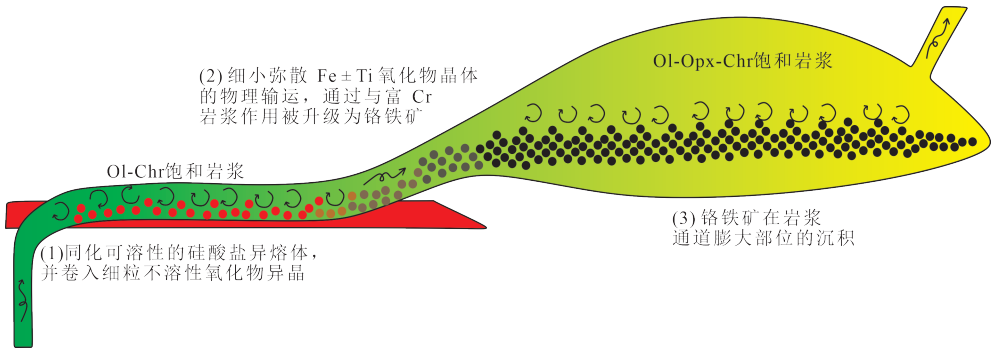


图10　埃及Dahanib阿拉斯加型杂岩体及其带状铬铁矿成因模型(据Khedr et al.,2020修编)

Fig.10　A cartoon for the formation of the banded chromitite deposit and the Dahanib Alaskan-type complex in Egypt (modified after Khedr et al.,2020)



矿物符号：Ol—橄榄石；Chr—铬铁矿；Opx—斜方辉石

图11 Fe±Ti氧化物动态升级成因模型(据Lesher et al.,2019修编)

Fig.11 Genetic model for the dynamic upgrading of Fe±Ti oxides (modified after Lesher et al.,2019)

et al.,2018)。质量平衡分析和高温高压矿物-熔体分配实验表明,在上地幔橄榄岩部分熔融条件下,Cr在尖晶石和辉石中为相容元素,因而在熔融过程中倾向滞留于残留地幔相,而进入熔体的Cr含量相对较低(Chabot and Agee,2003;Davis et al.,2013)。也就是说,在地球早期的壳幔分异过程中,Cr优先赋存于地幔中,为铬铁矿床提供了成矿物质的最初来源。华北克拉通层状岩体中铬铁岩的Re-Os同位素数据为此提供了关键地质年代学证据,其Re亏损年龄为2.5~3.0 Ga(夏琼霞等,2004),与吴福元等(1997)通过长英质岩石Nd模式年龄揭示的壳幔分异时间较为一致,进一步证实壳幔分异过程中Cr的选择性富集。此外,来自灶神星代表幔源堆晶的古铜无球粒陨石相对于代表壳源熔体的钙长辉长无球粒陨石显著富Cr,也指示Cr的分馏与再分配早在岩浆洋冷却结晶主导的早期壳幔分异阶段便已发生(Mandler and Elkins-Tanton,2013;Bonnand et al.,2016)。值得注意的是,地壳的锆石U-Pb年龄以及地幔硫化物和铂族矿物的Re-Os模式年龄都呈不规则分布,并在约1.2、1.9、2.7和3.3 Ga处出现峰值,表明地球在上述时期曾发生大规模壳幔分异作用(Pearson et al.,2007;Coggon et al.,2013)。且全球尺度的大规模壳幔分异事件在时间上与Scavia-Superia、Nuna和Rodinia等超级大陆旋回以及不同类型铬铁矿时空分布的分段节点大体吻合(图12a),指示铬铁矿的形成与深部地幔温度、岩石圈结构及构造机制转换密切相关。

在太古宙早期至中期(>2900 Ma), 地幔整体处于高温状态(图12b),高Mg超镁铁质岩浆活动频繁,绿岩带型铬铁矿如Ujaragssuit、Nuasahi-Sukinda、Newlands、Railway Block等集中产出于高Mg玄武岩-科马提岩系和超镁铁质-镁铁质杂岩中。此类矿床的铬尖晶石普遍具有高$Cr^{\#}$、高$Mg^{\#}$和低TiO_2特征(图4a、4b),寄主橄榄岩中橄榄石也表现出极高的Fo值,表明其母岩浆来源于高程度部分熔融的亏损地幔(Stowe,1994;Rollinson,1997;Mondal et al.,2006;Mukherjee et al.,2010)。此外,绿岩带中与铬铁矿共生的科马提岩及高Mg、低Ti的富硅火山岩(即玻安岩型)组合的地球化学特征(Dostal,2008;Polat,2011;Szilas et al.,2012;Sossi et al.,2016),共同指示早期俯冲-增生过程参与了大陆形成和地壳演化,且全球TTG中Ba含量的统计变化表明俯冲作用在太古宙早期可能仅为局部发生,而非全球同步启动(Huang et al.,2022)。综上所述,太古宙已存在局部类似现代板块构造体制的俯冲过程,但其热结构和时空连续性可能不同于现今全球性冷而深的俯冲(Huang et al.,2022)。而绿岩带型铬铁矿正是这一早期板块体制下,高温高Mg岩浆作用与深部亏损地幔演化耦合过程的直接记录。

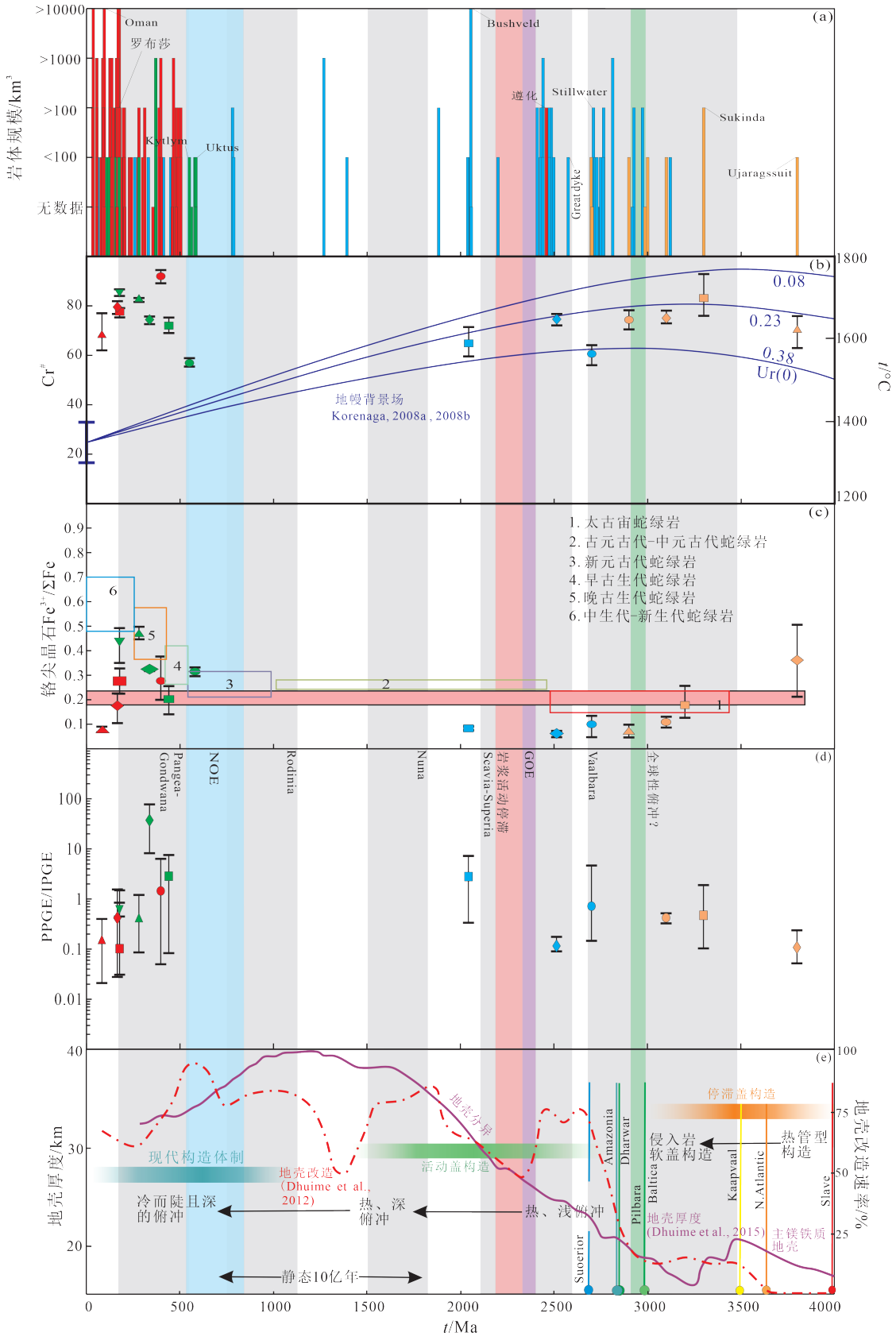
到晚太古代至早元古代(2800~2000 Ma), 2.7 Ga和1.9 Ga两次全球性Re亏损事件分别对应于Vaalabara与Superia-Sclavia超级大陆的聚合与裂解,伴随新生地壳增生速率与地壳改造程度的显著增强(图11e)(Maier and Groves,2011;Nance et al.,2014;Smith and Maier,2021)。在此背景下,幔源镁铁质岩浆通量显著增加,大规模底侵作用及下地壳岩浆储库更易发育,从而有利于形成体量巨大、寿命较长的岩浆房系统(Cawthorn,2005;Maier and Groves,2011)。与此同时,新生地壳的快速增生与改造可能削弱下地壳的热阻隔效应,并通过增强底侵与晶粥体系的热缓冲能力,使岩浆-晶粥系统在较长时间尺度内保持高温状态(Huppert and Sparks,1988;Annen et al.,2006),有利于形成层状铬铁矿。最早一期以Stillwater、Great Dyke为代表的层状铬铁矿的产出时代约为3.0~2.7 Ga,对应全球性俯冲启动时间之后、Superia-Sclavia等早期超级大陆聚合前的大规模幔源镁铁质岩浆活动阶段(Hawkesworth et al.,2010;Palin et al.,2020)。随后在大氧化事

表 3　全球主要铬铁矿床年龄对比表

Table 3　Comparison of ages of major chromitite deposits worldwide

矿床类型	矿床名称	成矿年龄/Ma	参考文献
层状铬铁矿	Bushveld(南非)	2043±11	Schoenberg et al.,1999
	Stillwater(美国)	2701±8	Marcantonio et al.,1993
	Great Dyke(津巴布韦)	2514±16	Oberthür et al.,2002;Wingate et al.,2000
	Kemi(芬兰)	2440 ±0.16	Manhès et al.,1980;Yang et al.,2016
	Muskox(加拿大)	1270±4	LeCheminant and Heaman,1989; Day et al.,2008
	Burakovsky(俄罗斯)	2433±4	Bailly et al.,2009
	Niquelandia(巴西)	1300~1250	Pimentel et al.,2004
	Ipueira-Medrado Sill(巴西)	2038±19	Oliveira and Lafon,1995;Marques et al.,2003
	Fiskenaesset(格陵兰岛)	2835±10	Pidgeon et al.,1976;Rollinson et al.,2002
	Bird River Sill(加拿大)	2745±5	Timmins et al.,1985
豆荚状铬铁矿	Kempirsai(哈萨克斯坦)	397±20	Edwards and Wasserburg,1985; Melcher et al.,1997
	Ray-IZ(俄罗斯)	485-470	Walker et al.,2002;Savelieva et al.,2006
	Guleman(土耳其)	82.0±2.9	Sapancı et al.,2023
	Bulqiza(阿尔巴尼亚)	164.8±3.1	Dilek et al.,2008
	Oman(阿曼)	95~94	Rioux et al.,2012
	罗布莎(中国西藏)	177±31	Shi et al.,2007
	Zambales(菲律宾)	44.2±0.9	Encarnación et al.,1993
	Troodos(塞浦路斯)	90.3±0.7	Büchl et al.,2004
	New Caledonia(美国)	34.3±0.3	Paquette and Cluzel,2007
	东巧(中国西藏)	177.7±2.2	Shi et al.,2007
阿拉斯加型铬铁矿	Duke Island(阿拉斯加)	118.5±1.5	Himmelberg and loney,1995
	Blasske Islands(阿拉斯加)	108~105	Himmelberg and loney,1995
	Goodnews Bay(阿拉斯加)	175~154	Himmelberg and loney,1995
	Kytlym(乌拉尔)	337±22	Zaccarini et al.,2018
	Nizhni Tagil(乌拉尔)	440~415	Tessalina et al.,2015
	Uktus(乌拉尔)	440~415	Garuti et al.,2003
	Tagil-Barancha(乌拉尔)	440~415	Garuti,2005
	Kondyor(俄罗斯)	176±1.2	Malitch et al.,2011
	Guli(俄罗斯)	370	Malitch et al.,2002,2011
	高寺台(中国)	280.3±2.9	Xiong et al.,2023
绿岩带型铬铁矿	Ujaragssuit(格陵兰)	~3800	Frei et al.,2002;Rollinson et al.,2002
	Nuasahi-Sukinda(印度)	3300~3100	Mondal et al.,2006,2019
	Aladahalli(印度)	3100	Mukherjee et al.,2010,2012
	Newlands(澳大利亚)	2900	Barnes and Jones,2013
	Railway Block(津巴布韦)	3000	Prendergast,2008
	Black Thor(加拿大)	2700	Scoates and Jon Scoates,2013
	Valley(津巴布韦)	3000	Prendergast,2008

件(GOE)之后的2.4~2.2 Ga期间,层状铬铁矿的地质记录出现明显空白,这与该时期岩浆活动停滞、地壳改造减弱以及地幔冷却加速的地球动力学背景相吻合(图12b、12e)(Condie et al.,2016),标志着全球板块构造动力体系的阶段性衰减。岩浆活动在2.1~2.0 Ga期间重新恢复活跃,从而在约2.05 Ga形成了目前已知世界上规模最大的Bushveld岩体及其相关小型含铬铁矿的层状侵入体。值得注意的是,该时期还存在极少数豆荚状铬铁矿的记录,如华北克拉通遵化蛇绿岩中豆荚状铬铁矿(约2550 Ma),其铬尖晶石内存在透辉石出溶片晶等



资料来源同表1、表2以及图中标注；Mosier等(2012)；Rollinson等(2017)；Bada和Korenaga(2018)；崔梦萌等(2020)；Smith 和 Maier(2021)；Huang等(2022)；Smith等(2024)

图12 地球演化过程中铬铁矿相关成分图解

Fig.12 Diagrams for compositions of chromitites in the Earth's evolution process

超高压指示特征,表明早在太古宙末期部分富Cr岩石圈地幔就已经能够随俯冲板片进入深部地幔甚至地幔过渡带,并在之后再次回返上地幔参与成矿(Hu et al.,2024)。此类古老记录虽然在全球范围内仍属个例,但从时间上将深俯冲-回返机制的起始推回至早太古代,为显生宙广泛发育的豆荚状铬铁矿所反映的再循环机制提供了重要先例和物质基础。

2000~800 Ma是地球演化过程中铬铁矿成矿的空白期,对应于地球演化过程中的"静态十亿年",其特征表现为构造活动的长期稳定、气候相对停滞以及生物演化速率趋缓(Santosh and Groves,2023),伴随被动大陆边缘数量减少(Bradley,2008)和弧岩浆作用减弱(Liu et al.,2019),从而导致与俯冲带相关的成矿作用总体减少(Santosh and Groves,2023)。尽管该时期有少数层状侵入体存在铬铁矿产出的报道,但多未达到工业品位,可能与大陆地盾内部放射性衰变热的持续降低有关—地热梯度显著下降,使岩浆在上升穿过冷而厚的大陆岩石圈过程中,难以维持足够高的Cr含量。此外,深地震剖面研究表明,中元古代大陆岩石圈明显加厚,并发育高速下地壳层(波速大于6.6 km/s),被普遍解释为大规模基性岩浆底侵或深部岩浆库强烈分异的产物(Durrheim and Mooney,1991),由此可推断大量Cr被封存于深部堆晶岩和岩石圈基底中。同时,实验研究表明,在铬铁矿饱和条件下,熔体中Cr含量对温度高度敏感,温度升高会显著提高熔体中的Cr含量(Murck and Campbell,1986;Roeder and Reynolds,1991),表明地幔温度的急剧下降可能会抑制地幔部分熔融形成高Cr熔体(图12b),从而导致全球范围内铬铁矿成矿进入显著低谷期。

新元古代以来,随着Rodinia超级大陆的裂解和Pangea-Gondwana超级大陆的聚合(Smith and Maier,2021),铬铁矿成矿活动再度增强,但成矿主导类型由层状铬铁矿转变为阿拉斯加型与豆荚状铬铁矿。与此同时,地壳厚度呈现降低的趋势,而地壳改造速率显著提高(图12e),且首次超过地壳增生速率(Dhuime et al.,2012,2015),反映板块构造体制由早期以内陆增生和大型岩浆房体系为主,逐步转变为以大陆边缘和冷而深俯冲带活动为主导的现代型板块构造格局(Hawkesworth et al.,2010;Nance et al.,2014)。在现代冷而深且陡的俯冲体系中,俯冲板片脱水及变质反应向上覆地幔楔持续输入富水且具有较高氧化能力的流体,使弧下岩浆体系相对于洋中脊岩浆普遍表现出更高的H_2O含量与更高的氧逸度(Kelley and Cottrell;2009;Evans,2012;Cottrell and Kelley,2013)。这种富水、高f_{O_2}的流体输入不仅改变了地幔楔的热结构和熔融方式,还促进了通量熔融在俯冲启动及弧前环境中的发生,从而有利于低Ti、高Mg弧前玄武岩-玻安岩系列熔体的生成(Pearce et al.,1984;Stern et al.,2012;Reagan et al.,2017),为弧前和岛弧环境中铬铁矿的大规模成矿提供了物质基础。

此外,新元古代以来与弧前-岛弧环境相关的样本整体分布于相对偏高的PPGE/IPGE区间(图12d),提示俯冲相关熔体-流体条件可能对PGE分配产生影响。同时,这一时期铬尖晶石的$Fe^{3+}/\Sigma Fe$整体升高,特别是在新元古代氧化事件之后,蛇绿岩和弧前橄榄岩明显向高氧逸度端演化(图12c),暗示俯冲板片携带的富水且相对氧化的流体与熔体,逐渐成为上覆地幔楔部分熔融和Cr富集的主要驱动力。其中阿拉斯加型铬铁矿多与岛弧环境中的超镁铁质和碱性杂岩体相关,豆荚状铬铁矿多集中产于蛇绿岩中的弧前橄榄岩和地幔楔残留体,表现为古生代至中生代沿缝合带及弧前、弧后构造带成带分布的大量中大型矿床。

综上所述,全球不同类型铬铁矿的时空分布与地球内部物质分异、超级大陆旋回以及地幔热状态和构造体制的长期演化高度耦合,其中太古宙绿岩带型铬铁矿记录了高温亏损地幔与早期俯冲增生过程下铬的初始富集;晚太古代至早元古代层状铬铁矿集中反映了大规模幔源岩浆活动和壳幔分异加强阶段,Cr在岩浆房及岩石圈基底中的再分配;而新元古代以来广泛发育的阿拉斯加型和豆荚状铬铁矿则体现了在冷而厚岩石圈背景下,俯冲板片输入的富水氧化流体作用影响下弧前与岛弧地幔楔中铬的再循环过程,整体表明铬铁矿成矿序列系统记录了地球壳幔演化和深部动力学格局转折的关键阶段。

作者贡献声明: 谢慧丹和熊发挥,研究构思和设计、数据收集、论文初稿撰写;桂维彬、龚小晗、何亮、邱添,论文写作与修订;徐向珍,数据整理和制图。

利益冲突声明: 作者保证本文无利益冲突。

致谢: 论文撰写过程中与山东科技大学孟元库教授进行了有益讨论,匿名审稿人提出了有益的意见和建议,在此一并致以诚挚的谢意。

参考文献(References):

Abdallah S E, Ali S, Obeid M A. 2019. Geochemistry of an Alaskan-type mafic-ultramafic complex in eastern desert, Egypt: New insights and constraints on the Neoproterozoic island arc magmatism. Geoscience Frontiers, 10(3): 941–955

Ahmed A H, Arai S. 2003. Platinum-group minerals in podiform chromitites of the Oman ophiolite. The Canadian Mineralogist, 41(3): 597–616

Ahmed A, Arai S. 2002. Unexpectedly high-PGE chromitite from the deeper

mantle section of the northern Oman ophiolite and its tectonic implications. Contributions to Mineralogy and Petrology, 143(3): 263–278

Aird H M, Ferguson K M, Lehrer M L, Boudreau A E. 2017. A study of the trace sulfide mineral assemblages in the Stillwater Complex, Montana, USA. Mineralium Deposita, 52(3): 361–382

Alapieti T T, Kujanpää J, Lahtinen J J, Papunen H. 1989. The Kemi stratiform chromitite deposit, northern Finland. Economic Geology, 84(5): 1057–1077

Ammannati E, Jacob D E, Avanzinelli R, Foley S F, Conticelli S. 2016. Low Ni olivine in silica-undersaturated ultrapotassic igneous rocks as evidence for carbonate metasomatism in the mantle. Earth and Planetary Science Letters, 444: 64–74

Amossé J, Dablé P, Allibert M. 2000. Thermochemical behaviour of Pt, Ir, Rh and Ru vs f_{O_2} and f_{S_2} in a basaltic melt. Implications for the differentiation and precipitation of these elements. Mineralogy and Petrology, 68(1): 29–62

Anders E, Grevesse N. 1989. Abundances of the elements: Meteoritic and solar. Geochimica et Cosmochimica Acta, 53(1): 197–214

Arai S, Ahmed A H. 2018. Secular change of chromite concentration processes from the Archean to the Phanerozoic. In: Processes and Ore Deposits of Ultramafic-Mafic Magmas through Space and Time. Amsterdam: Elsevier, 139–157

Arai S, Miura M, Tamura A, Akizawa N, Ishikawa A. 2020. Hydrothermal chromitites from the Oman ophiolite: The role of water in chromitite genesis. Minerals, 10(3): 217

Arai S, Miura M. 2016. Formation and modification of chromitites in the mantle. Lithos, 264: 277–295

Arai S. 1997. Control of wall-rock composition on the formation of podiform chromitites as a result of magma/peridotite interaction. Mining Geology, 47: 177–187

Arai S. 2013. Conversion of low-pressure chromitites to ultrahigh-pressure chromitites by deep recycling: A good inference. Earth and Planetary Science Letters, 379: 81–87

Augé T. 1987. Chromite deposits in the northern Oman ophiolite: Mineralogical constraints. Mineralium Deposita, 22(1): 1–10

Augé T, Genna A, Legendre O, Ivanov K S, Volchenko Y A. 2005. Primary platinum mineralization in the Nizhny Tagil and Kachkanar ultramafic complexes, Urals, Russia: A genetic model for PGE concentration in chromite-rich zones. Economic Geology, 100(4): 707–732

Azar B. 2010. The Blackbird chromite deposit, James Bay lowlands of Ontario, Canada: Implications for chromitite genesis in ultramafic conduits and open magmatic systems. Toronto, Canada: University of Toronto, 1–154

Bada J L, Korenaga J. 2018. Exposed areas above sea level on Earth> 3.5 Gyr ago: Implications for prebiotic and primitive biotic chemistry. Life, 8(4): 55

Bai W, Robinson P T, Fang Q, Yang J, Yan B, Zhang Z, Hu X F, Zhou M F, Malpas J. 2000. The pge and base-metal alloys in the podiform chromitites of the luobusa ophiolite, southern Tibet. The Canadian Mineralogist, 38(3): 585–598

Bai Y, Su B X, Chen C, Yang S H, Liang Z, Xiao Y, Qin K Z, Malaviarachchi S P K. 2017. Base metal mineral segregation and Fe-Mg exchange inducing extreme compositions of olivine and chromite from the Xiadong Alaskan-type complex in the southern part of the Central Asian Orogenic Belt. Ore Geology Reviews, 90: 184–192

Bailly L, Auge T, Cocherie A, Trofimov N N, Golubev A I, Tkachev A V, Cherkasov S V. 2009. New data on the age of the Burakovsky layered intrusion, Karelia. Doklady Earth Sciences, 426(1): 534–538

Ballhaus C, Wirth R, Fonseca R O C, Blanchard H, Pröll W, Bragagni A, Nagel T, Schreiber A, Dittrich S, Thome V, Hezel D C, Below R, Cieszynski H. 2017. Ultra-high pressure and ultra-reduced minerals in ophiolites may form by lightning strikes. Geochemical Perspectives Letters, 42–46

Barnes S J, Naldrett A J, Gorton M P. 1985. The origin of the fractionation of platinum-group elements in terrestrial magmas. Chemical Geology, 53(3–4): 303–323

Barnes S J, Naldrett A J. 1985. Geochemistry of the J-M (Howland) Reef of the Stillwater Complex, Minneapolis Adit area; I, Sulfide chemistry and sulfide-olivine equilibrium. Economic Geology, 80(3): 627–645

Barnes S J, Pagé P, Prichard H M, Zientek M L, Fisher P C. 2016. Chalcophile and platinum-group element distribution in the Ultramafic series of the Stillwater Complex, MT, USA: Implications for processes enriching chromite layers in Os, Ir, Ru, and Rh. Mineralium Deposita, 51(1): 25–47

Barnes S J, Roeder P L. 2001. The range of spinel compositions in terrestrial mafic and ultramafic rocks. Journal of Petrology, 42(12): 2279–2302

Barnes S, Jones S. 2013. Deformed chromitite layers in the coobina intrusion, pilbara craton, western Australia. Economic Geology, 108(2): 337–354

Bonnand P, Williams H M, Parkinson I J, Wood B J, Halliday A N. 2016. Stable chromium isotopic composition of meteorites and metal–silicate experiments: Implications for fractionation during core formation. Earth and Planetary Science Letters, 435: 14–21

Borisova A Y, Ceuleneer G, Kamenetsky V S, Arai S, Béjina F, Abily B, Bindeman I N, Polvé M, De Parseval P, Aigouy T, Pokrovski G S. 2012. A new view on the petrogenesis of the Oman ophiolite chromitites from microanalyses of chromite-hosted inclusions. Journal of Petrology, 53 (12): 2411–2440

Bradley D C. 2008. Passive margins through earth history. Earth-Science Reviews, 91(1–4): 1–26

Büchl A, Brügmann G, Batanova V G. 2004. Formation of podiform chromitite deposits: Implications from PGE abundances and Os isotopic compositions of chromites from the Troodos complex, Cyprus. Chemical Geology, 208(1–4): 217–232

Cai P J, Yang J S, Lian D Y, Wu W W, Yang Y, Rui H C. 2022. Knowledge structure and frontier evolution of research on chromitite: A scientometric review. Minerals, 12(10): 1211

Cameron E N. 1980. Evolution of the Lower Critical Zone, central sector, eastern Bushveld Complex, and its chromite deposits. Economic Geology, 75(6): 845–871

Cawthorn R G, Barnes S J, Ballhaus C, Malitch K N. 2005. Platinum group element, chromium, and vanadium deposits in mafic and ultramafic rocks. In: Hedenquist J W, Thompson J F H, Goldfarb R J, Richards J P (eds.). Economic Geology 100th Anniversary Volume. Littleton, Colorado: Society of Economic Geologists, 215–249

Chabot N L, Agee C B. 2003. Core formation in the Earth and Moon: New experimental constraints from V, Cr, and Mn. Geochimica et Cosmochi-

mica Acta, 67(11): 2077–2091

Chakraborty K L, Chakraborty T L. 1984. Geological features and origin of the chromite deposits of sukinda valley, Orissa, India. Mineralium Deposita, 19(4): 256–265

Chen C, De Hoog J C M, Su B X, Wang J, Uysal İ, Xiao Y. 2020. Formation process of dunites and chromitites in Orhaneli and Harmancık ophiolites (NW Turkey): Evidence from *in-situ* Li isotopes and trace elements in olivine. Lithos, 376–377: 105773

陈艳虹, 杨经绥. 2018. 豆荚状铬铁矿床研究回顾与展望. 地球科学, 43(4): 991–1010［Chen Y H, Yang J S. 2018. Formation of podiform chromitite deposits: Review and prospects. Earth Science 43(4): 991–1010 (in Chinese with English abstract)］

Coggon J A, Luguet A, Nowell G M, Appel P W U. 2013. Hadean mantle melting recorded by southwest Greenland chromitite ^{186}Os signatures. Nature Geoscience, 6(10): 871–874

Condie K C, Aster R C, van Hunen J. 2016. A great thermal divergence in the mantle beginning 2.5 Ga: Geochemical constraints from greenstone basalts and komatiites. Geoscience Frontiers, 7(4): 543–553

Cotterill P. 1969. The chromite deposits of Selukwe, Rhodesia. In: Wilson H D B (eds.). Magmatic Ore Deposits, A Symposium. Economic Geology Monograph, 4: 154–186.

Cottrell E, Kelley K A. 2013. Redox heterogeneity in mid-ocean ridge basalts as a function of mantle source. Science, 340(6138): 1314–1317

崔梦萌, 白洋, 罗扬, 苏本勋, 肖燕, 王静, 潘旗旗, 高东林. 2020. 阿拉斯加型岩体的基本特征、成岩过程及成矿作用. 矿床地质, 39(3): 397–418［Cui M M, Bai Y, Luo Y, Su B X, Xiao Y, Wang J, Pan Q Q, Gao D L. 2020. Characteristics, petrogenesis and metallogenesis of Alaskan-type complexes. Mineral Deposits, 39(3): 397–418 (in Chinese with English abstract)］

Das S, Basu A R, Mukherjee B K. 2017. In situ peridotitic diamond in Indus ophiolite sourced from hydrocarbon fluids in the mantle transition zone. Geology, 45(8): 755–758

Das S, Mukherjee B K, Basu A R, Sen K Jr. 2015. Peridotitic minerals of the Nidar Ophiolite in the NW Himalaya: Sourced from the depth of the mantle transition zone and above. In: Mukherjee S et al. (eds.). Tectonics of the Himalaya. London: Geological Society, 239–260

Davis F A, Humayun M, Hirschmann M M, Cooper R S. 2013. Experimentally determined mineral/melt partitioning of first-row transition elements (FRTE) during partial melting of peridotite at 3GPa. Geochimica et Cosmochimica Acta, 104: 232–260

Day J M D, Pearson D G, Hulbert L J. 2008. Rhenium–osmium isotope and platinum-group element constraints on the origin and evolution of the 1·27 Ga muskox layered intrusion. Journal of Petrology, 49(7): 1255–1295

De Hoog J C M, Gall L, Cornell D H. 2010. Trace-element geochemistry of mantle olivine and application to mantle petrogenesis and geothermobarometry. Chemical Geology, 270(1–4): 196–215

Dhuime B, Hawkesworth C J, Cawood P A, Storey C D. 2012. A change in the geodynamics of continental growth 3 billion years ago. Science, 335 (6074): 1334–1336

Dhuime B, Wuestefeld A, Hawkesworth C J. 2015. Emergence of modern continental crust about 3 billion years ago. Nature Geoscience, 8(7): 552–555

Dickey J S. 1975. A hypothesis of origin for podiform chromite deposits. Geochimica et Cosmochimica Acta, 39(6–7): 1061–1074

Dilek Y, Furnes H, Shallo M. 2008. Geochemistry of the Jurassic Mirdita Ophiolite (Albania) and the MORB to SSZ evolution of a marginal basin oceanic crust. Lithos, 100(1–4): 174–209

Dilek Y, Yang J S. 2018. Ophiolites, diamonds, and ultrahigh-pressure minerals: New discoveries and concepts on upper mantle petrogenesis. Lithosphere, 10(1): 3–13

Dobrzhinetskaya L F, Wirth R, Yang J, Green H W, Hutcheon I D, Weber P K, Grew E S. 2014. Qingsongite, natural cubic boron nitride: The first boron mineral from the Earth's mantle. American Mineralogist, 99(4): 764–772

Dostal J. 2008. Igneous rock associations 10. Komatiites. Geoscience Canada, 35(1): 21–31

Duke J M. 1982. Ore deposit model 7-Magma segregation deposits of chromite. Geochimica et Cosmochimica Acta, 39(6–7): 1061–1074

Durrheim R J, Mooney W D. 1991. Archean and Proterozoic crustal evolution: Evidence from crustal seismology. Geology, 19: 606–609

Eales H V, Botha W J, Hattingh P J, de Klerk W J, Maier W D, Odgers A T R. 1993. The mafic rocks of the Bushveld complex: A review of emplacement and crystallization history, and mineralization, in the light of recent data. Journal of African Earth Sciences (and the Middle East), 16(1–2): 121–142

Eales H V, Cawthorn R G. 1996. The bushveld complex. In: Layered Intrusions. Amsterdam: Elsevier, 181–229

Eales H V. 2000. Implications of the chromium budget of the western limb of the bushveld complex. South African Journal of Geology, 103(2): 141–150

Edwards R L, Wasserburg G J. 1985. The age and emplacement of obducted oceanic crust in the Urals from Sm-Nd and Rb-Sr systematics. Earth and Planetary Science Letters, 72(32): 389–404

Encarnación J P, Mukasa S B, Obille E C Jr. 1993. Zircon U-Pb geochronology of the Zambales and Angat Ophiolites, Luzon, Philippines: Evidence for an Eocene arc-back arc pair. Journal of Geophysical Research: Solid Earth, 98(B11): 19991–20004

El-Rahman Y A, Helmy H M, Shibata T, Yoshikawa M, Arai S, Tamura A. 2012. Mineral chemistry of the Neoproterozoic Alaskan-type Akarem Intrusion with special emphasis on amphibole: Implications for the pluton origin and evolution of subduction-related magma. Lithos, 155: 410–425

Evans B W, Frost B R. 1975. Chrome-spinel in progressive metamorphism: A preliminary analysis. Geochimica et Cosmochimica Acta, 39(6–7): 959–972

Evans K A. 2012. The redox budget of subduction zones. Earth-Science Reviews, 113(1–2): 11–32

Farré-de-Pablo J, Proenza J A, González-Jiménez J M, Garcia-Casco A, Colás V, Roqué-Rossell J, Camprubí A, Sánchez-Navas A. 2019. A shallow origin for diamonds in ophiolitic chromitites. Geology, 47(1): 75–78

Ferreira Filho C F, Araujo S M. 2009. Review of Brazilian chromite deposits associated with layered intrusions: Geological and petrological constraints for the origin of stratiform chromitites. Applied Earth Science, 118(3–4): 86–100

Frei R, Rosing M T, Waight T E, Ulfbeck D G. 2002. Hydrothermal-metasomatic and tectono-metamorphic processes in the Isua supracrustal belt (West Greenland): A multi-isotopic investigation of their effects on

the Earth's oldest oceanic crustal sequence. Geochimica et Cosmochimica Acta, 66(3): 467–486

Gamal El Dien H, Arai S, Doucet L S, Li Z X, Kil Y, Fougerouse D, Reddy S M, Saxey D W, Hamdy M. 2019. Cr-spinel records metasomatism not petrogenesis of mantle rocks. Nature Communications, 10: 5103

Garuti G, Proenza J A, Zaccarini F. 2007. Distribution and mineralogy of platinum-group elements in altered chromitites of the Campo Formoso layered intrusion (Bahia State, Brazil): Control by magmatic and hydrothermal processes. Mineralogy and Petrology, 89(3): 159–188

Garuti G, Pushkarev E V, Zaccarini F, Cabella R, Anikina E. 2003. Chromite composition and platinum-group mineral assemblage in the Uktus Uralian-Alaskan-type complex (Central Urals, Russia). Mineralium Deposita, 38(3): 312–326

Garuti G, Pushkarev E V, Zaccarini F. 2002. Composion and paragenesis of Pt Alloys from Chromitites of the Uralian-Alaskan-type and Uktus complexes, Northern and central Urals, Russia. The Canadian Mineralogist, 40: 1127–1146

Garuti G, Pushkarev E, Thalhammer O A R, Zaccarini F. 2012. Chromitites of the Urals (Part 1): Overview of chromite mineral chemistry and geotectonic setting. Ofioliti, 37(1), 27–53

Garuti G, Zaccarini F, Moloshag V, Alimov V. 1999. Platinum-group minerals as indicator of sulfur fugacity in ophiolitic upper mantle: An example from chromitites of the Ray-Iz ultramafic complex, Polar Urals, Russia. The Canadian Mineralogist, 37(5): 1099–1115

González-Jiménez J M, Griffin W L, Gervilla F, Proenza J A, O'Reilly S Y, Pearson N J. 2014a. Chromitites in ophiolites: How, where, when, why Part I. A review and new ideas on the origin and significance of platinum-group minerals. Lithos, 189: 127–139

González-Jiménez J M, Griffin W L, Proenza J A, Gervilla F, O'Reilly S Y, Akbulut M, Pearson N J, Arai S. 2014b. Chromitites in ophiolites: How, where, when, why Part II. The crystallization of chromitites. Lithos, 189: 140–158

González-Jiménez J M, Kerestedjian T, Proenza J A, Gervilla F. 2009. Metamorphism on chromite ores from the dobromirtsi ultramafic Massif, Rhodope Mountains (SE Bulgaria). Geologica Acta, 7(4): 413–429

Grammatikopoulos T A, Kapsiotis A, Tsikouras B, Hatzipanagiotou K, Zaccarini F, Garuti G. 2011. Spinel composition, pge geochemistry and mineralogy of the chromitites from the vourinos ophiolite complex, northwestern Greece. The Canadian Mineralogist, 49(6): 1571–1598

Greenbaum D. 1977. The chromitiferous rocks of the Troodos ophiolite complex, Cyprus. Economic Geology, 72(7): 1175–1194

Griffin W L, Afonso J C, Belousova E A, Gain S E, Gong X H, González-Jiménez J M, Howell D, Huang J X, McGowan N, Pearson N J, Satsukawa T, Shi R, Williams P, Xiong Q, Yang J S, Zhang M, O'Reilly S Y. 2016b. Mantle recycling: Transition zone metamorphism of Tibetan ophiolitic peridotites and its tectonic implications. Journal of Petrology, 57(4): 655–684

Griffin W L, Gain S E M, Adams D T, Huang J X, Saunders M, Toledo V, Pearson N J, O'Reilly S Y. 2016a. First terrestrial occurrence of tistarite (Ti_2O_3): Ultra-low oxygen fugacity in the upper mantle beneath Mount Carmel, Israel. Geology 44, 815–818

Hamilton J. 1977. Sr isotope and trace element studies of the great dyke and bushveld mafic phase and their relation to Early Proterozoic magma genesis in southern Africa. Journal of Petrology, 18(1): 24–52

Hart S R, Davis K E. 1978. Nickel partitioning between olivine and silicate melt. Earth and Planetary Science Letters, 40(2): 203–219

Hawkesworth C J, Dhuime B, Pietranik A B, Cawood P A, Kemp A I S, Storey C D. 2010. The generation and evolution of the continental crust. Journal of the Geological Society, 167(2): 229–248

Hayes B, Maghdour-Mashhour R, Ashwal L D, Smith A J B, Ueckermann H, Vermeulen J. 2025. Melt infiltration in a crystal mush and pegmatoid formation in the platiniferous Merensky Reef, Bushveld Complex, South Africa. Mineralium Deposita, 60: 237–259

Himmelberg G R, Loney R A. 1995. Characteristics and petrogenesis of Alaskan-type ultramafic-mafic intrusions, southeastern Alaska. Washington: U.S. Geological Survey, 1–47

Hu W, Wang L, Kusky T, Chen T. 2024. To the transition zone and back: Records from diopside exsolution lamellae in chromite from Archean ophiolitic podiform chromitites. Earth and Planetary Science Letters, 625: 118475

Huang G Y, Mitchell R N, Palin R M, Spencer C J, Guo J H. 2022. Barium content of Archaean continental crust reveals the onset of subduction was not global. Nature Communications, 13: 6553

Huang M X, Yang J J, Powell R, Mo X. 2014. High-pressure metamorphism of serpentinized chromitite at Luobusha (southern Tibet). American Journal of Science, 314(1): 400–433

Huang Z, Yang J S, Robinson P T, Zhu Y W, Xiong F H, Liu Z, Zhang Z M, Xu W. 2015. The discovery of diamonds in chromitites of the hegenshan ophiolite, Inner Mongolia, China. Acta Geologica Sinica (English Edition), 89(2): 341–350

Hulbert L J, Von Gruenewaldt G. 1985. Textural and compositional features of chromite in the lower and critical zones of the Bushveld Complex south of Potgietersrus. Economic Geology, 80(4): 872–895

Huppert H E, Sparks R S J. 1988. The generation of granitic magmas by intrusion of basalt into continental crust. Journal of Petrology, 29(3): 599–624

Irvine T N. 1967. Chromian spinel as a petrogenetic indicator: Part 2. Petrologic applications. Canadian Journal of Earth Sciences, 4(1): 71–103

Irvine T N. 1974. Petrology of the duke island ultramafic complex southeastern Alaska. In: 138: Petrology of the Duke Island Ultramafic Complex Southeastern Alaska. Geological Society of America, 1–244

Irvine T N. 1975. Crystallization sequences in the Muskox intrusion and other layered intrusions: II. Origin of chromitite layers and similar deposits of other magmatic ores. Geochimica et Cosmochimica Acta, 39(6–7): 991–1020

Irvine T N. 1977. Origin of chromitite layers in the Muskox intrusion and other stratiform intrusions: A new interpretation. Geology, 5(5): 273

Jackson E D. 1968. The chromite deposits of the Stillwater Complex, Montana. In: Ridge J D (ed.). Ore Deposits of the United States, 1933–1967 (Graton-Sales Volume). New York: American Institute of Mining, Metallurgical, and Petroleum Engineers, 1495–1510

Jenkins M C, Mungall J E. 2018. Genesis of the Peridotite Zone, Stillwater Complex, Montana, USA. Journal of Petrology, 59(11): 2157–2189

Kelemen P B, Shimizu N, Salters V J M. 1995. Extraction of mid-ocean-ridge basalt from the upwelling mantle by focused flow of melt in dunite channels. Nature, 375(6534): 747–753

Kelley K A, Cottrell E. 2009. Water and the oxidation state of subduction zone magmas. Science, 325(5940): 605–607

Khedr M Z, Arai S, Morishita T. 2020. Formation of banded chromitites and associated sulphides in the Neoproterozoic subarc deep-crustal magma inferred from the Alaskan-type complex, Egypt. Ore Geology Reviews, 120: 1–26

Khedr M Z, Arai S. 2016. Petrology of a Neoproterozoic Alaskantype complex from the eastern desert of Egypt: Implications for mantle heterogeneity. Lithos, 263: 15–32

Klock W, Palme H. 1988. Partitioning of siderophile and chalcophile elements between sulfide, olivine, and glass in a naturally reduced basalt from Disko Island, Greenland. In: Ryder G, Sharpton V L (eds.). Proceedings of the 18th Lunar and Planetary Science Conference. Houston, Texas, USA, March 16–20, 1987. Houston: Lunar and Planetary Institute, 471–483

Korenaga J. 2008a. Plate tectonics, flood basalts, and the evolution of Earth's oceans. Terra Nova, 20(6): 419–439

Korenaga J. 2008b. Urey ratio and the structure and evolution of Earth's mantle. Reviews of Geophysics, 46(2): RG2007

Krause J, Brügmann G E, Pushkarev E V. 2007. Accessory and rock forming minerals monitoring the evolution of zoned mafic–ultramafic complexes in the Central Ural Mountains. Lithos, 95(1–2): 19–42

Lago B L, Rabinowicz M, Nicolas A. 1982. Podiform chromite ore bodies: A genetic model. Journal of Petrology, 23(1): 103–125

Langa M M, Jugo P J, Leybourne M I, Grobler D F, Adetunji J, Skogby H. 2021. Chromite chemistry of a massive chromitite seam in the northern limb of the Bushveld Igneous Complex, South Africa: Correlation with the UG-2 in the eastern and western limbs and evidence of variable assimilation of footwall rocks. Mineralium Deposita, 56: 1455–1472

Latypov R, Chistyakova S, Mukherjee R. 2017. A novel hypothesis for origin of massive chromitites in the bushveld igneous complex. Journal of Petrology, 58(10): 1899–1940

Latypov R, Costin G, Chistyakova S, Hunt E J, Mukherjee R, Naldrett T. 2018. Platinum-bearing chromite layers are caused by pressure reduction during magma ascent. Nature Communications, 9: 462

LeCheminant A N, Heaman L M. 1989. Mackenzie igneous events, Canada: Middle Proterozoic hotspot magmatism associated with ocean opening. Earth and Planetary Science Letters, 96(1–2): 38–48

Lee C A. 1996. A review of mineralization in the bushveld complex and some other layered intrusions. In: Layered Intrusions. Amsterdam: Elsevier, 103–145

Lenaz D, Garuti G, Zaccarini F, Cooper R W, Princivalle F. 2012. The Stillwater Complex: The response of chromite crystal chemistry to magma injection. Geologica Acta, 10(1): 33–41

Li Chusi, Ripley E M. 2010. The relative effects of composition and temperature on olivine-liquid Ni partitioning: Statistical deconvolution and implications for petrologic modeling. Chemical Geology, 275(1–2): 99–104

Lesher C M, Carson H J E, Houlé M G. 2019. Genesis of chromite deposits by dynamic upgrading of Fe ± Ti oxide xenocrysts. Geology, 47(3): 207–210

Lian D Y, Yang J S, Wiedenbeck M, Dilek Y, Rocholl A, Xiong F H, Wu W W. 2017. Origin of peridotites and chromitites in the pozanti-kar santi ophiolite, Turkey. Acta Geologica Sinica (English Edition), 91(s1): 15

Lipin B R. 1993. Pressure increases, the formation of chromite seams, and the development of the ultramafic series in the stillwater complex, Montana. Journal of Petrology, 34(5): 955–976

Liu H, Sun W D, Zartman R, Tang M. 2019. Continuous plate subduction marked by the rise of alkali magmatism 2.1 billion years ago. Nature Communications, 10: 3408

Lorand J P, Ceuleneer G. 1989. Silicate and base-metal sulfide inclusions in chromites from the Maqsad area (Oman ophiolite, Gulf of Oman): A model for entrapment. Lithos, 22(3): 173–190

Maier W D, Groves D I. 2011. Temporal and spatial controls on the formation of magmatic PGE and Ni–Cu deposits. Mineralium Deposita, 46(8): 841–857

Malitch K N, Badanina I Y. 2015. Iron-platinum alloys from chromitites of the Nizhny Tagil and Kondyor clinopyroxenite-dunite massifs (Russia). Doklady Earth Sciences, 462(2): 634–637

Malitch K N, Puchtel I S, Belousova E A, Badanina I Y. 2020. Contrasting platinum-group mineral assemblages of the Kondyor massif (Russia): Implications for the sources of HSE in zoned-type ultramafic massifs. Lithos, 376: 105800

Mandler B E, Elkins-Tanton L T. 2013. The origin of eucrites, diogenites, and olivine diogenites: Magma ocean crystallization and shallow magma chamber processes on Vesta. Meteoritics & Planetary Science, 48(11): 2333–2349

Manhès G, Allègre C J, Dupré B, Hamelin B. 1980. Lead isotope study of basic-ultrabasic layered complexes: Speculations about the age of the Earth and primitive mantle characteristics. Earth and Planetary Science Letters, 47(3): 370–382

Marcantonio F, Zindler A, Reisberg L, Mathez E A. 1993. Re-Os isotopic systematics in chromitites from the Stillwater Complex, Montana, USA. Geochimica et Cosmochimica Acta, 57(16): 4029–4037

Marques J C, Dias J R P, Friedrich B M, Frantz J C, Queiroz W J A, Botelho N F. 2017. Thick chromitite of the Jacurici Complex (NE Craton São Francisco, Brazil): Cumulate chromite slurry in a conduit. Ore Geology Reviews, 90: 131–147

Marques J C, Ferreira Filho C F, Carlson R W, Pimentel M M. 2003. Re–Os and Sm–Nd isotope and trace element constraints on the origin of the chromite deposit of the ipueira–medrado sill, Bahia, Brazil. Journal of Petrology, 44(4): 659–678

Marques J C, Filho C F F. 2003. The chromite deposit of the Ipueira-Medrado sill, São Francisco Craton, Bahia State, Brazil. Economic Geology, 98(1): 87–108

McCallum I S. 1996. The stillwater complex: A review of the Geology. In: Layered Intrusions. Amsterdam: Elsevier, 441–483

McDonald J A. 1965. Liquid immiscibility as one factor in chromitite seam formation in the Bushveld igneous complex. Economic Geology, 60(8): 1674–1685

Melcher F, Grum W, Simon G, Thalhammer T V, Stumpfl E F. 1997. Petrogenesis of the ophiolitic giant chromite deposits of kempirsai, Kazakhstan: A study of solid and fluid inclusions in chromite. Journal of Petrology, 38(10): 1419–1458

Molebale J I. 2011. Characterization of platinum group minerals in the UG-2 chromitite layer, north eastern Bushveld Complex, South Africa. South Africa: University of Pretoria, 1–116

Mondal S K, Khatun S, Prichard H M, Satyanarayanan M, Ravindra Kumar G

R. 2019. Platinum-group element geochemistry of boninite-derived Mesoarchean chromitites and ultramafic-mafic cumulate rocks from the Sukinda Massif (Orissa, India). Ore Geology Reviews, 104: 722–744

Mondal S K, Mathez E A. 2007. Origin of the UG2 chromitite layer, bushveld complex. Journal of Petrology, 48(3): 495–510

Mondal S K, Ripley E M, Li C S, Frei R. 2006. The genesis of Archaean chromitites from the Nuasahi and Sukinda massifs in the Singhbhum Craton, India. Precambrian Research, 148(1–2): 45–66

Mondal S K. 2009. Chromite and PGE deposits of mesoarchaean ultramafic-mafic suites within the greenstone belts of the Singhbhum craton, India: Implications for mantle heterogeneity and tectonic setting. Journal of the Geological Society of India, 73(1): 36–51

Mosier D L, Singer D A, Moring B C and Galloway L P. 2012. Podiform chromite deposits—database and grade and tonnage models. Reston: U.S. Geological Survey, 1–54

Mukherjee R, Mondal S K, Frei R, Rosing M T, Waight T E, Zhong H, Ravindra Kumar G R. 2012. The 3.1Ga Nuggihalli chromite deposits, Western Dharwar craton (India): Geochemical and isotopic constraints on mantle sources, crustal evolution and implications for supercontinent formation and ore mineralization. Lithos, 155: 392–409

Mukherjee R, Mondal S K, Rosing M T, Frei R. 2010. Compositional variations in the Mesoarchean chromites of the Nuggihalli schist belt, Western Dharwar Craton (India): Potential parental melts and implications for tectonic setting. Contributions to Mineralogy and Petrology, 160 (6): 865–885

Murck B W, Campbell I H. 1986. The effects of temperature, oxygen fugacity and melt composition on the behaviour of chromium in basic and ultrabasic melts. Geochimica et Cosmochimica Acta, 50(9): 1871–1887

Naldrett A J, Wilson A, Kinnaird J, Yudovskaya M, Chunnett G. 2012. The origin of chromitites and related PGE mineralization in the Bushveld Complex: New mineralogical and petrological constraints. Mineralium Deposita, 47(3): 209–232

Nance R D, Murphy J B, Santosh M. 2014. The supercontinent cycle: A retrospective essay. Gondwana Research, 25(1): 4–29

Nekrasov I Y, Lennikov A M, Zalishchak B L, Oktyabrsky R A, Ivanov V V, Sapin V I, Taskaev V I. 2005. Compositional variations in platinum-group minerals and gold, konder alkaline-ultrabasic massif, Aldan shield, Russia. The Canadian Mineralogist, 43(2): 637–654

Nicolas A, Al Azri H. 1990. Chromite-rich and chromite-poor ophiolites: The Oman case. In: Ophiolite Genesis and Evolution of the Oceanic Lithosphere. Dordrecht: Springer Netherlands, 5: 261–274

Nicolas A, Prinzhofer A. 1983. Cumulative or residual origin for the transition zone in ophiolites: Structural evidence. Journal of Petrology, 24(2): 188–206

Nishio I, Morishita T, Waterton P, Tamura A, Itano K, Serre S H, Plesner J L, Takahashi K, Tani K, Harigane Y, Sawada H, Szilas K. 2025. Komatiitic parental magmas of the Archean Ujaragssuit Nunât ultramafic body, SW Greenland, identified from spinel chemistry. Contributions to Mineralogy and Petrology, 180(3): 20

O'Driscoll B, González-Jiménez J M. 2016. Petrogenesis of the platinum-group minerals. Reviews in Mineralogy and Geochemistry, 81(1): 489–578

Oberthür T, Davis D W, Blenkinsop T G, Höhndorf A. 2002. Precise U–Pb mineral ages, Rb–Sr and Sm–Nd systematics for the Great Dyke, Zimbabwe: Constraints on late Archean events in the Zimbabwe craton and Limpopo belt. Precambrian Research, 113(3–4): 293–305

Oberthür T, Weiser T W, Gast L, Kojonen K. 2003. Geochemistry and mineralogy of platinum-group elements at Hartley Platinum Mine, Zimbabwe: Part 1. Primary distribution patterns in pristine ores of the Main Sulfide Zone of the Great Dyke. Mineralium Deposita, 38(3): 327–343

Oliveira E P, Lafon J M. 1995. Idade dos Complexos máficoultramáficos mineralizados de Caraíba e Medrado, Bahia, por evaporação de Pb em zircão. Congresso Brasileiro de Geoquímica, 5th, Niterói, 1995

Özkan Y Z. 1982. Structural investigation of Guleman (Elazığ) ophiolites. Bulletin of the Mineral Research and Exploration, 97: 32–39

Page N J, Engin T, Singer D A, Haffty J. 1984. Distribution of platinum-group elements in the Bati Kef chromite deposit, Guleman-Elazig area, eastern Turkey. Economic Geology, 79(1): 177–184

Paktunc A D. 1990. Origin of podiform chromite deposits by multistage melting, melt segregation and magma mixing in the upper mantle. Ore Geology Reviews, 5(3): 211–222

Palin R M, Santosh M, Cao W T, Li S S, Hernández-Uribe D, Parsons A. 2020. Secular change and the onset of plate tectonics on Earth. Earth-Science Reviews, 207: 103172

Paquette J L, Cluzel D. 2007. U–Pb zircon dating of post-obduction volcanic-arc granitoids and a granulite-facies xenolith from New Caledonia. Inference on Southwest Pacific geodynamic models. International Journal of Earth Sciences, 96(4): 613–622

Pearce J A, Lippard S J, Roberts S. 1984. Characteristics and tectonic significance of supra-subduction zone ophiolites. Geological Society, London, Special Publications, 16(1): 77–94

Pearson D G, Parman S W, Nowell G M. 2007. A link between large mantle melting events and continent growth seen in osmium isotopes. Nature, 449(7159): 202–205

Peyerl W. 1982. The influence of the Driekop dunite pipe on the platinum-group mineralogy of the UG-2 chromitite in its vicinity. Economic Geology, 77(6): 1432–1438

Pidgeon R T, Aftalion M, Kalsbeek F. 1976. The age of the Ilivertalik granite in the Fiskenæsset area. Rapport Grønlands Geologiske Undersøgelse, 73: 31–33

Pimentel M M, Filho C F F, Armstrong R A. 2004. SHRIMP U-Pb and Sm-Nd ages of the Niquelândia layered complex: Meso- (1.25 Ga) and Neoproterozoic (0.79 Ga) extensional events in central Brazil. Precambrian Research, 132(1–2): 133–153

Polat A, Appel P W U, Fryer B J. 2011. An overview of the geochemistry of Eoarchean to Mesoarchean ultramafic to mafic volcanic rocks, SW Greenland: Implications for mantle depletion and petrogenetic processes at subduction zones in the early Earth. Gondwana Research, 20(2–3): 255–283

Polat A, Frei R, Schersten A, Appel P W U. 2010. New age (ca. 2970 Ma), mantle source composition and geodynamic constraints on the Archean Fiskenæsset anorthosite complex, SW Greenland. Chemical Geology, 277 (1–2): 1–20

Prendergast M D. 2008. Archean komatiitic sill-hosted chromite deposits in the Zimbabwe craton. Economic Geology, 103(5): 981–1004

Prichard H M, Barnes S J, Fisher P C, Pagé P, Zientek M L. 2017. Laurite and associated PGM in the stillwater chromitites: Implications for processes of formation, and comparisons with laurite in the bushveld and ophiolitic chromitites. The Canadian Mineralogist, 55(1): 121–144

Qiu T, Yang J S, Milushi I, Wu weiei, Mekshiqi N, Xiong F H, Zhang C, Shen T T. 2019. Petrogenesis and PGE abundances of high-Cr and high-Al chromitites and peridotites from the bulqiza ultramafic massif, eastern mirdita ophiolite, Albania. Acta Geologica Sinica (English Edition), 93 (S2): 25

Reagan M K, Pearce J A, Petronotis K, Almeev R R, Avery A J, Carvallo C, Chapman T, Christeson G L, Ferré E C, Godard M. 2017. Subduction initiation and ophiolite crust formation: Insights from IODP drilling in the western Pacific. Lithosphere, 9(5): 688–710

Rioux M, Bowring S, Kelemen P, Gordon S, Dudás F, Miller R. 2012. Rapid crustal accretion and magma assimilation in the Oman-U.A.E. ophiolite: High precision U-Pb zircon geochronology of the gabbroic crust. Journal of Geophysical Research: Solid Earth, 117: B07201

Rizeli M E, Bingöl A F, Wang K L, Lee H Y. 2023. Abyssal and forearc features of mantle peridotites in the Guleman ophiolite in SE Turkey. Lithos, 436–437: 106958

Robb L. 2020. Introduction to ore-forming processes. 2nd. Hoboken: John Wiley & Sons, 1–496

Robinson P T, Bai Wenji, Malpas J, Yang Jingsui, Zhou Meifu, Fang Qingsong, Hu Xufeng, Cameron S, Staudigel H. 2004. Ultra-high pressure minerals in the Luobusa Ophiolite, Tibet, and their tectonic implications. Geological Society, London, Special Publications, 226: 247–271

Robinson P T, Trumbull R B, Schmitt A, Yang J S, Li J W, Zhou M F, Erzinger J, Dare S, Xiong F H. 2015. The origin and significance of crustal minerals in ophiolitic chromitites and peridotites. Gondwana Research, 27 (2): 486–506

Roeder P L, Reynolds I. 1991. Crystallization of chromite and chromium solubility in basaltic melts. Journal of Petrology, 32(5): 909–934

Rollinson H, Appel P W U, Frei R. 2002. A metamorphosed, early Archaean chromitite from west Greenland: Implications for the genesis of Archaean anorthositic chromitites. Journal of Petrology, 43(11): 2143–2170

Rollinson H. 1997. The Archean komatiite-related inyala chromitite, southern Zimbabwe. Economic Geology, 92(1): 98–107

Rollinson H. 2005. Chromite in the mantle section of the Oman ophiolite: A new genetic model. Island Arc, 14(4): 542–550

Rollinson H, Adetunji J, Lenaz D, Szilas K. 2017. Archaean chromitites show constant $Fe^{3+}/\Sigma Fe$ in Earth's asthenospheric mantle since 3.8 Ga. Lithos, 282-283: 316–325

Rui H C, Yang J S, Llanes Castro A I, Zheng J P, Lian D Y, Wu W W, Valdés Mariño Y. 2022. Ti-poor high-Al chromitites of the Moa-Baracoa ophiolitic massif (eastern Cuba) formed in a nascent forearc mantle. Ore Geology Reviews, 144: 104847

Saha A K. 1994. Crustal evolution of Singhbhum North Orissa, Eastern India. Geological Society of India Memoir, 27: 1–341

Santosh M, Groves D I. 2023. The Not-So-Boring Billion: A metallogenic conundrum during the evolution from Columbia to Rodinia super-continents. Earth-Science Reviews, 236: 104287

Sapancı Ö, Tokat G, Eraslan N K, Karakaya A O, Ali Gücer M, Çimen O. 2023. Geochemical and radiometric data for mafic rocks from the Guleman Ophiolite (SE, Turkey): New insights on the geodynamic evolution of the southern Neo-Tethyan ocean. Lithos, 442: 107071

Saveliev D E, Makatov D K, Vishnevskiy A V, Gataullin R A. 2023. Accessory minerals in the chromitite ores of dzharlybutak ore group of kempirsai massif (southern urals, Kazakhstan): Clues for ore genesis. Minerals, 13 (2): 263

Savelieva G N, Suslov P V, Larionov A N, Berezhnaya N G. 2006. Age of zircons from chromites in the residual ophiolitic rocks as a reflection of upper mantle magmatic events. Doklady Earth Sciences, 411(2): 1401–1406

Sawada H, Morishita T, Vezinet A, Stern R, Tani K, Nishio I, Takahashi K, Graham Pearson D, Szilas K. 2023. Zircon within chromitite requires revision of the tectonic history of the Eoarchean Itsaq Gneiss complex, Greenland. Geoscience Frontiers, 14(6): 101648

Schoenberg R, Kruger F J, Nägler T F, Meisel T, Kramers J D. 1999. PGE enrichment in chromitite layers and the Merensky Reef of the western Bushveld Complex; a Re–Os and Rb-Sr isotope study. Earth and Planetary Science Letters, 172(1–2): 49–64

Schouwstra R P, Kinloch E D, Lee C A. 2000. A short geological review of the bushveld complex. Platinum Metals Review, 44(1): 33–39

Schulte R F, Taylor R D, Piatak N M, Seal R R. 2012. Stratiform chromite deposit model. II. Resto: U.S. Geological Survey, 1–148

Scoates J S, Jon Scoates R F. 2013. Age of the bird river sill, southeastern Manitoba, Canada, with implications for the secular variation of layered intrusion-hosted stratiform chromite mineralization. Economic Geology, 108(4): 895–907

Sharkov E V, Bogatikov O A, Grokhovskaya T L, Chistyakov A V, Ganin V A, Grinevich N G, Snyder G A, Taylor L A. 1995. Petrology and Ni-Cu-Cr-PGE mineralization of the largest mafic pluton in Europe: The Early Proterozoic burakovsky layered intrusion, Karelia, Russia. International Geology Review, 37(6): 509–525

Shi R D, Alard O, Zhi X C, O'Reilly S Y, Pearson N J, Griffin W L, Zhang M, Chen X M. 2007. Multiple events in the Neo-Tethyan oceanic upper mantle: Evidence from Ru-Os-Ir alloys in the Luobusa and Dongqiao ophiolitic podiform chromitites, Tibet. Earth and Planetary Science Letters, 261(1–2): 33–48

Shi R D, Griffin W L, O'Reilly S Y, Huang Q S, Zhang X R, Liu D L, Zhi X C, Xia Q X, Ding L. 2012. Melt/mantle mixing produces podiform chromite deposits in ophiolites: Implications of Re-Os systematics in the Dongqiao Neo-Tethyan ophiolite, northern Tibet. Gondwana Research, 21(1): 194–206

Sigurdsson H, Schilling J G. 1976. Spinels in mid-Atlantic ridge basalts: Chemistry and occurrence. Earth and Planetary Science Letters, 29(1): 7–20

Smith W D, Maier W D. 2021. The geotectonic setting, age and mineral deposit inventory of global layered intrusions. Earth-Science Reviews, 220: 103736

Sossi P A, Eggins S M, Nesbitt R W, Nebel O, Hergt J M, Campbell I H, St C O'Neill H, Van Kranendonk M, Davies D R. 2016. Petrogenesis and geochemistry of Archean komatiites. Journal of Petrology, 57(1): 147–184

Spandler C, Mavrogenes J, Arculus R. 2005. Origin of chromitites in layered

intrusions: Evidence from chromite-hosted melt inclusions from the Stillwater Complex. Geology, 33(11): 893

Stern R J, Reagan M, Ishizuka O, Ohara Y, Whattam S. 2012. To understand subduction initiation, study forearc crust: To understand forearc crust, study ophiolites. Lithosphere, 4(6): 469–483

Stowe C W. 1994. Compositions and tectonic settings of chromite deposits through time. Economic Geology, 89(3): 528–546

Su B X, Chen Y, Mao Q, Zhang D, Jia L H, Guo S. 2019. Minor elements in olivine inspect the petrogenesis of orogenic peridotites. Lithos, 344: 207–216

Su B X, Jing J J. 2025. Super-reduced and ultra-high pressure minerals in ophiolites: A critical review and the case for meteorite impact. Earth-Science Reviews, 270: 105228

Su B X. 2022. Cretaceous meteorite impact-induced initial subduction: Records of highly siderophile element abundances and Re-Os isotopes in ophiolites. Journal of Earth Science, 33(6): 1526–1534

苏本勋, 白洋, 陈晨, 刘霞, 肖燕, 唐冬梅, 梁子, 崔梦萌, 彭青山. 2018. 铬铁矿床母岩浆含水性的岩石矿物学探讨. 矿物岩石地球化学通报, 37(6): 1035–1046［Su B X, Bai Y, Chen C, Liu X, Xiao Y, Tang D M, Liang Z, Cui M M, Peng Q S. 2018. Petrological and mineralogical investigations on hydrous properties of parental magmas of chromite deposits. Bulletin of Mineralogy, Petrology and Geochemistry, 37(6): 1035–1046 (in Chinese with English abstract)］

苏本勋, 刘霞, 陈晨, Paul T.ROBINSON, 肖燕, 周美夫, 白洋, Ibrahim UYSAL, 张鹏飞. 2021. 蛇绿岩铬铁矿成矿新模型: 流体不混溶作用. 中国科学: 地球科学, 51(2): 250–260［Su B X, Liu X, Chen C, Robinson P T, Xiao Y, Zhou M, Bai Y, Uysal I, Zhang P. 2021. A new model for chromitite formation in ophiolites: Fluid immiscibility. Scientia Sinica (Terrae), 51(2): 250–260 (in Chinese with English abstract)］

孙凯, 赵志丹, 柯珊, 何胜飞, 周肃, 任军平, 吴兴源, 古阿雷. 2019. 津巴布韦大岩墙层状铬铁矿地球化学特征及地质意义. 地质与勘探, 55(01): 103–114［Sun K, Zhao Z D, Ke S, He S F, Zhou S, Ren J P, Wu X Y. 2019. Geochemistry and geological significance of the layered chromite in the Great Dyke of Zimbabwe. Geology and exploration, 55(1): 103–114 (in Chinese with English abstract)］

Szilas K, Næraa T, Scherstén A, Stendal H, Frei R, van Hinsberg V J, Kokfelt T F, Rosing M T. 2012. Origin of Mesoarchaean arc-related rocks with boninite/komatiite affinities from southern West Greenland. Lithos, 144–145: 24–39

Talkington R W, Lipin B R. 1986. Platinum-group minerals in chromite seams of the Stillwater Complex, Montana. Economic Geology, 81(5): 1179–1186

Taylor H P. 1967. The zoned ultramafic complexes of southeastern Alaska. New York: John Wiley and Sons Incorporated, 97–121

Tessalina S G, Malitch K N, Augé T, Puchkov V N, Belousova E, McInnes B I A. 2015. Origin of the nizhny Tagil clinopyroxenite–dunite massif, Uralian platinum belt, Russia: Insights from PGE and Os isotope systematics. Journal of Petrology, 56(12): 2297–2318

Thakurta J, Ripley E M, Li C S. 2008. Geochemical constraints on the origin of sulfide mineralization in the Duke Island Complex, southeastern Alaska. Geochemistry, Geophysics, Geosystems, 9(7): Q11006

Thakurta J. 2018. Alaskan-type complexes and their associations with economic mineral deposits. In: Mondal S K, Griffin W L (eds.). Processes and ore deposits of ultramafic-mafic magmas through space and time. Amsterdam: Elsevier, 269–302

Thayer T P. 1964. Principal features and origin of podiform chromite deposits, and some observations on the Guelman-Soridag District, Turkey. Economic Geology, 59(8): 1497–1524

Tian W, Chen B, Ireland T R, Green D H, Suzuki K, Chu Z. 2011. Petrology and geochemistry of dunites, chromitites and mineral inclusions from the Gaositai Alaskan-type complex, North China Craton: Implications for mantle source characteristics. Lithos, 127: 165–175

Tian Y Z, Yang J S, Robinson P T, Xiong F H, Li Y, Zhang Z M, Liu Z, Liu F, Niu X L. 2015. Diamond discovered in high-Al chromitites of the sartohay ophiolite, Xinjiang province, China. Acta Geologica Sinica (English Edition), 89(2): 332–340

Timmins E A, Turek A, Symons D T A, Smith P E. 1985. U-Pb zircon geochronology and paleomagnetism of the Bird River greenstone belt, Manitoba. In: Program with Abstracts, Mineralogical Association of Canada Joint Annual Meeting, 1985. Geological Association of Canada, 10: A62

Tsomondo J M. 1995. The Shurugwi chromite deposits: New perspectives and exploration outlook. Geological Society of Zimbabwe, Special Publication, 3: 25–37

Ulmer G C. 1969. Experimental investigations of chromite spinels. In: Magmatic Ore Deposits. Society of Exploration Geophysicists Geophysical Monograph 4. Tulsa: Society of Economic Geologists, 114–131

Uysal I, Kapsiotis A, Akmaz R M, Saka S, Seitz H M. 2018. The Guleman ophiolitic chromitites (SE Turkey) and their link to a compositionally evolving mantle source during subduction initiation.Ore Geology Reviews, 93: 98–113

Veksler I V, Sedunova A P, Darin A V, Anosova M O, Reid D L, Kaufmann F E D, Hecht L, Trumbull R B. 2018. Chemical and textural re-equilibration in the UG2 chromitite layer of the Bushveld Complex, South Africa. Journal of Petrology, 59(6): 1193–1216

Voordouw R J, Gutzmer J, Beukes N J. 2010. Zoning of platinum group mineral assemblages in the UG2 chromitite determined through *in situ* SEM-EDS-based image analysis. Mineralium Deposita, 45(2): 147–159

Voordouw R, Gutzmer J, Beukes N J. 2009. Intrusive origin for Upper Group (UG1, UG2) stratiform chromitite seams in the Dwars River area, Bushveld Complex, South Africa. Mineralogy and Petrology, 97(1): 75–94

Walker R J, Prichard H M, Ishiwatari A, Pimentel M. 2002. The osmium isotopic composition of convecting upper mantle deduced from ophiolite chromites. Geochimica et Cosmochimica Acta, 66(2): 329–345

Wang J, Su B X, Robinson P T, Xiao Y, Bai Y, Liu X, Sakyi P A, Jing J J, Chen C, Liang Z, Bao Z A. 2021. Trace elements in olivine: Proxies for petrogenesis, mineralization and discrimination of mafic-ultramafic rocks. Lithos, 388: 106085

王嘉玮, 蔡鹏捷, SZILAS Kristoffer, 连东洋, 杨经绥. 2023. 太古宙绿岩带中铬铁矿床研究现状与展望. 岩石学报, 39(12): 3734–3758［Wang J W, Cai P J, Kristoffer S, Lian D Y, Yang J S. 2023. A review and outlook on Archean greenstone belt-hosted chromite deposits. Acta Petrologica Sinica, 39(12): 3734–3758 (in Chinese with English abstract)］

Wang Z L, Yan J Y, Zheng X M, Tang H J, Yuan L L, Deng Z, Fang T H. 2023. Formation and evolution of chromitites in the Hongshishan complex,

Beishan Orogenic collage, NW China: Constraints from mineralogical compositions, Re-Os isotopes and platinum-group element geochemistry. Acta Geologica Sinica (English Edition), 97(3): 727–743

Wilson A H. 1996. The Great Dyke of Zimbabwe. In: Layered Intrusions. Amsterdam: Elsevier, 365–402

Windley B F. 1995. The Evolving Continents. 3rd Edition. Singapore: John Wiley & Sons, 441–443

Wingate M T D. 2000. Ion microprobe U: Pb zircon and baddeleyite ages for the Great Dyke and its satellite dykes, Zimbabwe. South African Journal of Geology, 103(1): 74–80

吴福元, 葛文春, 孙德有, 林强, 周燕. 1997. 吉林南部太古代花岗岩Sm-Nd, Rb-Sr同位素年龄测定. 岩石学报, 13(4): 499–506［Wu F Y, Ge W C, Sun D Y, Lin Q, Zhou Y. 1997. The Sm Nd, Rb Sr isotopic ages of the Archean granites in southern Jilin Province. Acta Petrologica Sinica, 13 (4): 499–506 (in Chinese with English abstract)］

Wu W W, Yang J S, Ma C Q, Milushi I, Lian D Y, Tian Y Z. 2017. Discovery and significance of diamonds and moissanites in chromitite within the skenderbeu massif of the mirdita zone ophiolite, west Albania. Acta Geologica Sinica (English Edition), 91(3): 882–897

夏琼霞, 支霞臣, 李江海, 黄雄南. 2004. 新太古代球粒陨石型对流上地幔: 河北遵化豆荚状铬铁矿的Os同位素组成. 科学通报, 49(24): 2587–2591［Xia Q X, Zhi X C, Li J H, Huang X N. 2004. Neoarchean chondrite convective upper mantle: Os isotopic composition of podiform chromite in Zunhua, Hebei Province. Chinese Science Bulletin, 49(24): 2587–2591 (in Chinese with English abstract)］

谢慧丹, 龚小晗, 何亮, 穆小平, 徐向珍, 邱添, 桂维彬, 杨经绥, 熊发挥. 2025. 班公湖-怒江缝合带蛇绿岩特征对比与铬铁矿的前景讨论. 地质学报, 99(11): 3664–3686［Xie H D, Gong X H, He L, Mu X P, Xu X Z, Qiu T, Gui W B, Yang J S, Xiong F H. 2025. Discussion regarding the characteristic comparison of ophiolites within the Bangongco-Nujiang suture zone and the prospects for chromite deposits. Acta Geologica Sinica, 99(11): 3664–3686 (in Chinese with English abstract)］

熊发挥,杨经绥,刘钊. 2013. 豆荚状铬铁矿多阶段形成过程的讨论. 中国地质, 40(3): 820–839［Xiong F H, Yang J S, LIU Z. 2013. Multi-satge formation of the podiform chromitite. Geology in China, 40(3): 820–839 (in Chinese with English abstract)］

Xiong F H, Yang J S, Dilek Y, Xu X Z, Zhang Z M. 2017. Origin and significance of diamonds and other exotic minerals in the Dingqing ophiolite peridotites, eastern Bangong-Nujiang suture zone, Tibet. Lithosphere, 10(1): 142–155

Xiong F H, Yang J S, Paul R T, Xu X Z, Ba D Z, Li Y, Li J Y, Zhang Z M, Rong H. 2016. Diamond discovered in Dangqiong ophiolite, western Yarlung-zangbu suture zone, Tibet. Acta Geologica Sinica (English Edition), 89(s2): 99–100

Xiong F H, Yang J S, Robinson P T, Dilek Y, Milushi I, Xu X Z, Chen Y H, Zhou W D, Zhang Z M, Lai S M, Tian Y Z, Huang Z. 2015. Petrology and geochemistry of high $Cr^{\#}$ podiform chromitites of Bulqiza, Eastern Mirdita Ophiolite (EMO), Albania. Ore Geology Reviews, 70: 188–207

Xiong F H, Yang J S, Robinson P T, Xu X Z, Liu Z, Li Y, Li J Y, Chen S Y. 2015. Origin of podiform chromitite, a new model based on the Luobusa ophiolite, Tibet. Gondwana Research, 27(2): 525–542

Xiong F H, Zoheir B, Li C, Xu X Z, Qiu T, Benaouda R, Chen J. 2023. Atypical chromitite deposit in the Gaositai mafic-ultramafic complex, North China Craton: Geochemical, geochronological, and isotopic systematics. Lithos, 460: 107388

Xiong F H, Xu Xiangzhen, Mugnaioli E, Gemmi M, Wirth R, Grew E S, Robinson R T, Yang Jingsui. 2020b. Two new minerals, badengzhuite (TiP) and zhiqinite ($TiSi_2$), from the Cr-11 chromitite orebody, Luobusa ophiolite, Tibet, China: Is this evidence for super-reduced mantle-derived fluids. European Journal of Mineralogy, 32(5): 557–574

Xiong F H, Zoheir B, Robinson P T, Yang J S, Xu X Z, Meng F C. 2020a. Genesis of the Ray-Iz chromitite, Polar Urals: Inferences to mantle conditions and recycling processes. Lithos, 354–355: 105699

Xiong F H, Zoheir B, Wirth R, Milushi I, Qiu T, Yang J S. 2021. Mineralogical and isotopic peculiarities of high-Cr chromitites: Implications for a mantle convection genesis of the Bulqiza ophiolite. Lithos, 398: 106305

Xiong F H, Zoheir B, Xu X Z, Guo G L, Frische M, Yang J S. 2024. Geochemical characteristics of mineral inclusions in the Luobusa chromitite (Southern Tibet): Implications for an intricate geological setting. American Mineralogist, 109(12): 2127–2141

Xiong F H, Zoheir B, Xu X Z, Qiu T, Gui W B, Xie H D, Yang J S. 2025. Role of mantle dynamics and geochemical diversity in chromitite formation: insights from the Luobusa ophiolite, SW Tibet. Mineralium Deposita, 60: 1689–1712

Xu X Z, Yang J S, Chen S Y, Fang Q S, Bai W J, Ba D Z. 2009. Unusual mantle mineral group from chromitite orebody Cr-11 in Luobusa ophiolite of Yarlung-Zangbo suture zone, Tibet. Journal of Earth Science, 20(2): 284–302

Xu X Z, Yang J S, Robinson P T, Xiong F H, Ba D Z, Guo G L. 2015. Origin of ultrahigh pressure and highly reduced minerals in podiform chromitites and associated mantle peridotites of the Luobusa ophiolite, Tibet. Gondwana Research, 27(2): 686–700

Xu X Z, Zoheir B, Yang J S, Xiong F H, Guo G L, Feng G Y, Li Z L, Li T F. 2023. Tectonized Neotethyan lithosphere in southeastern Tibet: Results of the Luobusa ophiolite drilling. Lithos, 436: 106947

徐向珍, 杨经绥, 熊发挥, 郭国林. 2018. 罗布莎豆荚状铬铁矿床中刚玉的含Ti矿物包裹体特征. 地球科学, 43(4): 1025–1037［Xu X Z, Yang J S, Xiong F H, Guo G L. 2018. Characteristics of titanium-bearing inclusions found in corundum of luobusa podiform chromitite, Tibet. Earth Science, 43(4): 1025–1037 (in Chinese with English abstract)］

Yamamoto S, Komiya T, Hirose K, Maruyama S. 2009. Coesite and clinopyroxene exsolution lamellae in chromites: *In-situ* ultrahigh-pressure evidence from podiform chromitites in the Luobusa ophiolite, southern Tibet. Lithos, 109(3–4): 314–322

Yang F, Santosh M, Tsunogae T, Tang L, Teng X M. 2017. Multiple magmatism in an evolving suprasubduction zone mantle wedge: The case of the composite mafic–ultramafic complex of Gaositai, North China Craton. Lithos, 284: 525–544

Yang J J, Zhang H R, Chen A P, Huang M X. 2017. Petrological evidence for shock-induced high-P metamorphism in a gabbro. Journal of Metamorphic Geology, 35(2): 121–140

Yang J S, Dobrzhinetskaya L, Bai W J, Fang Q S, Robinson P T, Zhang J F, Green H W. 2007. Diamond- and coesite-bearing chromitites from the luobusa ophiolite, Tibet. Geology, 35(10): 875

Yang J S, Meng F C, Xu X Z, Robinson P T, Dilek Y, Makeyev A B, Wirth R, Wiedenbeck M, Cliff J. 2015. Diamonds, native elements and metal alloys

from chromitites of the Ray-Iz ophiolite of the Polar Urals. Gondwana Research, 27(2): 459–485

Yang J S, Wu W W, Lian D Y, Rui H C. 2021. Peridotites, chromitites and diamonds in ophiolites. Nature Reviews Earth & Environment, 2(3): 198–212

杨经绥, 巴登珠, 徐向珍, 李兆丽. 2010. 中国铬铁矿床的再研究及找矿前景. 中国地质, 37(4): 1141–1150［Yang J S, Ba D Z, Xu X Z, Li Z L. 2010. A restudy of podiform chromite deposits and their ore-prospecting vista in China. Geology in China, 37(4): 1141–1150 (in Chinese with English abstract)］

杨经绥, 徐向珍, 张仲明, 戎合, 李源, 熊发挥, 梁凤华, 刘钊, 刘飞, 李金阳, 李兆丽, 陈松永, 郭国林, Paul ROBINSON. 2013. 蛇绿岩型金刚石和铬铁矿深部成因. 地球学报, 34(6): 643–653［Yang J S, Xu X Z, Zhang Z M, Rong H, Li Y, Xiong F H, Liang F H, Liu Z, Liu F, Li J Y, Li Z L, Chen S Y, Guo G L, Robinson P. 2013. Ophiolite-type diamond and deep genesis of chromitite. Acta Geoscientica Sinica, 34(6): 643–653 (in Chinese with English abstract)］

杨经绥. 2020. 大洋地幔橄榄岩-铬铁矿中的金刚石和深地幔再循环. 地质力学学报, 26(5): 731–741［Yang J S. 2020. Diamond in oceanic peridotites-chromitites and recycled in deep mantle. Journal of Geomechanics, 26(5): 731–741 (in Chinese with English abstract)］

Yang S H, Hanski E, Li C, Maier W D, Huhma H, Mokrushin A V, Latypov R, Lahaye Y, O'Brien H, Qu W J. 2016. Mantle source of the 2.44–2.50-Ga mantle plume-related magmatism in the Fennoscandian Shield: Evidence from Os, Nd, and Sr isotope compositions of the Monchepluton and Kemi intrusions. Mineralium Deposita, 51(8): 1055–1073

Yurichev A N, Chernyshov A I, Korbovyak E V. 2019. Platinum group minerals from chromitites of Kempirsai ultramafic massif (the South Urals): New data. Zapiski RMO (Proceedings of the Russian Mineralogical Society), 148(2): 76–86

Zaccarini F, Economou-Eliopoulos M, Tsikouras B, Garuti G. 2024. Chromite Composition and Platinum-Group Elements Distribution in Tethyan Chromitites of the Mediterranean Basin: An Overview. Minerals, 14(8): 744

Zaccarini F, Garuti G, Pushkarev E V. 2011. Unusually PGE-rich chromitite in the Butyrin vein of the Kytlym Uralian–Alaskan complex, northern Urals, Russia. The Canadian Mineralogist, 49(6): 1413–1431

Zaccarini F, Garuti G, Pushkarev E, Thalhammer O. 2018. Origin of platinum group minerals (PGM) inclusions in chromite deposits of the urals. Minerals, 8(9): 379

Zaccarini F, Pushkarev E, Garuti G, Krause J, Dvornik G P, Stanley C, Bindi L C. 2013. Platinum-group minerals (PGM) nuggets from alluvial-eluvial placer deposits in the concentrically zoned mafic-ultramafic Uktus complex (Central Urals, Russia). European Journal of Mineralogy, 25 (4): 519–531

翟明国. 2022. 太古宙的洋-陆与古地理问题. 古地理学报, 24(5): 825–847［Zhai M G. 2022. Ocean and continent in Archean. Journal of Palaeogeography (Chinese Edition), 24(5): 825–847 (in Chinese with English abstract)］

Zhang P F, Zhou M F, Yumul G P Jr, Liu D Y, Li X H, Li Q L. 2020. Coexistence of high-Al and high-Cr chromite orebodies in the Acoje block of the Zambales ophiolite, Philippines: Evidence for subduction initiation. Ore Geology Reviews, 125: 103660

张泽南, 张照志, 潘昭帅, 吴晴, 徐恒逸. 2019. 全球铬矿石资源国对中国供应安全度分析. 中国矿业, 28(10): 69–76［Zhang Z N, Zhang Z Z, Pan Z S, Wu Q, Xu H Y. 2019. Analysis of China's supply safety by global chromium ore resource countries. China Mining Magazine, 28(10): 69–76 (in Chinese with English abstract)］

赵金召, 董培培, 郭菁华, 王帅, 张夏炜, 宋珈璐. 2025. 河北高寺台超基性杂岩体中铬铁矿特征及地质意义. 资源环境与工程, 39(2): 171–177［Zhao J Z, Dong P P, Guo Q H, Wang S, Zhang X W, Song J L. 2025. Characteristics and geological significance of chromite in Gaositai ultrabasic complex, Hebei Province. Resources Environment & Engineering, 39(2): 171–177 (in Chinese with English abstract)］

Zhou M F, Robinson P T, Bai W J. 1994. Formation of podiform chromitites by melt/rock interaction in the upper mantle. Mineralium Deposita, 29(1): 98–101

Zhou M F, Robinson P T, Malpas J, Li Z J. 1996. Podiform chromitites in the Luobusa ophiolite (southern Tibet): Implications for melt-rock interaction and chromite segregation in the upper mantle. Journal of Petrology, 37(1): 3–21

Zhou M F, Robinson P T, Su B X, Gao J F, Li J W, Yang J S, Malpas J. 2014. Compositions of chromite, associated minerals, and parental magmas of podiform chromite deposits: The role of slab contamination of asthenospheric melts in suprasubduction zone environments. Gondwana Research, 26(1): 262–283

Zhou M F, Sun M, Keays R R, Kerrich R W. 1998. Controls on platinum-group elemental distributions of podiform chromitites: A case study of high-Cr and high-Al chromitites from Chinese Orogenic belts. Geochimica et Cosmochimica Acta, 62(4): 677–688

Zhukova I A, Stepanov A S, Jiang S Y, Zhimulev F I, Gurevich D V, Polonyankin A A, Lavrenchuk A V, Kotlyarov A. 2025. Platinum-group elements geochemistry of chromite from Kondyor ultramafic intrusion, Siberia: re-evaluation of factors controlling PGE content of intrusive chromite. Chemical Geology, 691: 122871

Zirakparvar N A, Mathez E A, Rajesh H M, Choe S. 2019. Lu-Hf isotopic evidence of a deep mantle plume source for the 2.06 Ga Bushveld Large Igneous Province. Lithos, 348: 105168